Submitted to SISC; accepted November 2013.

A SPACE-TIME PETROV-GALERKIN CERTIFIED REDUCED BASIS METHOD: APPLICATION TO THE BOUSSINESQ EQUATIONS

MASAYUKI YANO*

Abstract. We present a space-time certified reduced basis method for long-time integration of parametrized parabolic equations with quadratic nonlinearity which admit an affine decomposition in parameter but with no restriction on coercivity of the linearized operator. We first consider a finite element discretization based on discontinuous Galerkin time integration and introduce associated Petrov-Galerkin space-time trial- and test-space norms that yield optimal and asymptotically mesh independent stability constants. We then employ an *hp* Petrov-Galerkin (or minimum residual) space-time reduced basis approximation. We provide the Brezzi-Rappaz-Raviart *a posteriori* error bounds which admit efficient *offline-online* computational procedures for the three key ingredients: the dual norm of the residual, an inf-sup lower bound, and the Sobolev embedding constant. The latter are based respectively on a more round-off resistant residual norm evaluation procedure, a variant of the successive constraint method, and a time-marching implementation of a fixed-point iteration of the embedding constant for the discontinuous Galerkin norm. Finally, we apply the method to a natural convection problem governed by the Boussinesq equations. The result indicates that the space-time formulation enables rapid and certified characterization of moderate-Grashof-number flows exhibiting steady periodic responses. However, the space-time reduced basis convergence is slow, and the Brezzi-Rappaz-Raviart threshold condition is rather restrictive, such that offline effort will be acceptable only for very few parameters.

Key words. space-time Petrov-Galerkin, parametrized parabolic equations, discontinuous Galerkin, certified reduced basis, Brezzi-Rappaz-Raviart theory, Boussinesq equations

AMS subject classifications.

1. Introduction.

We present a certified reduced basis (CRB) method for long-time integration of parametrized parabolic partial differential equations (PDEs) with quadratic nonlinearity which admit an affine decomposition in parameter but with no restriction on coercivity of the linearized operator.[1] Our equations of interest include, but are not limited to, the unsteady incompressible Navier-Stokes equations and the Boussinesq equations that exhibit moderate unsteadiness including time-periodic responses. While reduced basis *approximation* based on, for example, proper orthogonal decomposition (POD) readily applies to unsteady equations [12, 13], *certification* based on traditional time-marching $L^2(\Omega)$ error bounds has been shown to be ineffective when the spatial operator linearized about the solution trajectory is non-coercive [19, 16]. In particular, the time-marching $L^2(\Omega)$ error bound — which is based on the consideration of the worst-case perturbation at each time step and the propagation of its effect over time — grows exponentially in time for non-coercive (linearized) spatial operator even if the solution is asymptotically stable (and steady).

In order to overcome the limitation of the time-marching $L^2(\Omega)$ error bound and enable effective long-time *certification* of a reduced basis approximation of non-coercive (but asymptotically stable) PDEs, Urban and Patera have recently introduced an error bound based on a space-time variational formulation [25, 24]. Instead of accumulating the effect of the worst-case perturbation at each time step, the formulation directly considers the space-time structure of the problem and con-

*Department of Mechanical Engineering, Massachusetts Institute of Technology, Cambridge, MA 02139, USA (myano@mit.edu)

[1] We assume that the first term of the decomposition of the linear term is positive and symmetric; the precise mathematical form of the assumption is provided in Section 2.1.

structs a space-time error bound. For spatially non-coercive and asymptotically stable convection-diffusion equations, the formulation has been shown (empirically) to yield an error bound that grows linearly, rather than exponentially, with the final time.

More recently, we (Yano, Urban, and Patera) have applied the space-time approximation and error certification technique in a simple nonlinear setting: one-parameter, one-dimensional Burgers' equation [28]. The work employed an interpolation-based reduced basis approximation and the associated Brezzi-Rappaz-Raviart (BRR) error bound [3] specialized for quadratic nonlinearity (as used by Veroy and Patera for steady Navier-Stokes [26]). The primary advantage of the formulation in [28] is its simplicity in many aspects: the Crank-Nicolson in time truth discretization, the reduced basis approximation (in fact, interpolation), the inf-sup stability bound, and the sampling procedure.[2] The method however has a number of disadvantages: a (stringent) restriction on the form of the equation — the linearized form must be independent of the parameter; the weak stability of the natural space-time norm associated with the Crank-Nicolson time-stepping; the associated poor behavior of the Sobolev embedding constant (which is required for the BRR error bound); and the non-optimality of the interpolation-based (as oppose to projection-based) reduced-basis approximation. Nevertheless the simple formulation demonstrated the applicability of the space-time formulation for Burgers' equation and significant improvement in the effectivity of the error bound compared to the time-marching formulation.

The point of departure for the current work is the above work on Burgers' equation [28]. Our new formulation improves upon previous approach in several regards. First, we relax the constraint that the linearized form is independent of the parameter; specifically, we consider equations whose linear and quadratic spatial operators admit decompositions that are affine in functions of parameter. (Again, we assume that the first term of the decomposition of the linear term is positive and symmetric in the sense defined in Section 2.1; the diffusion term of the parabolic equation constitutes this operator.) Second, we employ a new "truth" space-time finite element discretization based on the discontinuous Galerkin (DG) time stepping [15, 10] and introduce associated space-time trial and test norms, which yield unity inf-sup and continuity constants for the heat equation and produce a L^4 embedding constant that is only weakly dependent on the mesh and final time. Third, we employ an *hp* Petrov-Galerkin projection-based (or minimum residual) reduced basis approximation [18] instead of the interpolation-based approximation used in the previous work, facilitating applicability of the method in a multi-parameter setting. Fourth, we use a modified version of natural-norm successive constraint method [14] in the space-time context that provides a tighter bound than the original formulation while maintaining a similar cost for nonlinear equations. Fifth, we present a variant of the *hp*-adaptive reduced basis sampling strategy [9] that is particularly suited for nonlinear equations with limited stability. Finally, we apply the new space-time certified reduced basis formulation to a natural convection problem governed by the unsteady Boussinesq equations — a system for which the classical time-marching $L^2(\Omega)$ error bound produces pessimistic and meaningless error bounds.

We however note that the space-time CRB method proposed in this work suffers from a number of limitations that warrant future work. The first is the disadvantage of space-time snapshots relative to POD-Greedy approaches in terms of the convergence of the reduced-basis approximation and hence offline effort; future work will consider

[2] Due to its simplicity, in particular from an implementation perspective, certain aspects of the formulation in [28] may be preferred in some cases.

how we may incorporate a POD-Greedy *approximation* into a space-time *certification*. The second is the very restrictive (normalized) residual criterion imposed by the Brezzi-Rappaz-Raviart theory, which in turn requires a very accurate reduced basis approximation ("overkill") before we can endow the solution with *any* error certificate; it might be difficult to address this from a purely computational perspective, but in an estimation or controls context — one of the target applications of reduced basis methods — data may help to mitigate the effect. We will observe both of these limitations in our model Boussinesq equations.

The results nevertheless demonstrate that rigorous long-time *a posteriori* error bounds are possible for unsteady and "unstable"[3] hydrodynamic and transport systems. The natural convection system considered in the results section exhibits qualitatively different responses as the Grashof number increases: from a Stokes-like smooth transition at a low Grashof number to a convection-dominated steady-periodic response at a high Grashof number. The method is able to rigorously confirm that these changes in flow regime are not the result of an overly truncated low-order model, which is a demonstrated danger in a reduced-order approximation of unsteady flows [7]. With the space-time formulation we achieve rigorous bound (by avoiding spurious dynamics), but to achieve this rigor, we do not lose the sharpness.

This paper is organized as follows. Section 2 introduces a space-time variational and finite element formulation based on a discontinuous Galerkin time-marching and associated space-time trial and test norms. Section 3 presents our space-time certified reduced basis framework. The section describes the construction of the reduced basis approximation and the three ingredients of the BRR-based error certification: the dual norm of the residual, a inf-sup constant lower bound, and a Sobolev embedding constant. Section 4 presents our *hp*-adaptive reduced basis sampling strategy. Finally, Section 5 shows the result of applying the space-time certified reduced basis method to a laterally heated natural convection problem.

2. Truth Solution.

2.1. Problem Description. Let us first recall a few standard spaces that are used throughout this work [20]. The L^2 Hilbert space over a domain $\Omega \in \mathbb{R}^d$ is denoted by $L^2(\Omega)$ and is equipped with an inner product $(\psi,\phi)_{L^2(\Omega)} \equiv \int_\Omega \phi(x)\psi(x)dx$ and the induced norm $\|\psi\|_{L^2(\Omega)} \equiv \sqrt{(\psi,\psi)_{L^2(\Omega)}}$. The space of vector valued $L^2(\Omega)$ functions is denoted by $(L^2(\Omega))^m$, where m is the dimension of vectors, and is equipped with an inner product $(\xi,\eta)_{L^2(\Omega)} \equiv \int_\Omega \eta_j(x)\xi_j(x)dx = \sum_{j=1}^m (\xi_j,\eta_j)_{L^2(\Omega)}$ and the induced norm $\|\xi\|_{L^2(\Omega)} \equiv \sqrt{(\xi,\xi)_{L^2(\Omega)}}$; to avoid notational clutter, we will not explicitly indicate in the subscript that inner product (or norm) is taken in the vector sense. The summation on repeated indices is implied throughout this paper unless stated otherwise; however, we will employ the explicit summation notation when the limit of summation is ambiguous. The L^p norm is defined by $\|\psi\|_{L^p(\Omega)} \equiv \left(\int_\Omega (\sum_{j=1}^m \psi_j(x)\psi_j(x))^{p/2}dx\right)^{1/p}$. The $H^1(\Omega)$ space is equipped with an inner product $(\psi,\phi)_{H^1(\Omega)} \equiv (\nabla\psi,\nabla\phi)_{L^2(\Omega)}$ and the induced norm $\|\psi\|_{H^1(\Omega)} \equiv \sqrt{(\psi,\psi)_{H^1(\Omega)}}$. We will also consider Gelfand triple (V,H,V') and associated duality pairing $\langle\cdot,\cdot\rangle_{V'\times V}$; we take $H = L^2(\Omega)$ (or $(L^2(\Omega))^m$) throughout this work and appropriately choose V to suit the equation of interest. The norm of $\ell \in V'$ is defined by $\|\ell\|_{V'} \equiv \sup_{\psi\in V}\langle\ell,\psi\rangle_{V'\times V}/\|\psi\|_V$. The Riesz representation $R\ell \in V$ satisfies $\|R\ell\|_V = \|\ell\|_{V'}$, where the Riesz operator is defined as $R : V' \to V$ such that, for each $\ell \in V'$, $(R\ell,\phi)_V = \langle\ell,\phi\rangle_{V'\times V}$, $\forall\phi \in V$.

[3] In the sense of having a non-coercive (linearized) spatial operator.

We now introduce the form of governing equation considered in this work. Let $\Omega \subset \mathbb{R}^d$ be the spatial domain, $I = (0,T]$ be the time interval, and $\mathcal{D} \subset \mathbb{R}^P$ be the parameter domain. We consider parametrized quadratically-nonlinear parabolic equations of the following form: find $u \in C^0(I;H) \cap L^2(I;V)$ such that [20, 22]

$$(\dot{u}, v)_H + a(u, v; \mu) + c(u, u, v; \mu) = f(v; \mu), \quad \forall v \in V,\, t \in I,\, \mu \in \mathcal{D}, \tag{2.1}$$
$$(u(0), \eta)_H = (h(\mu), \eta)_H, \quad \forall \eta \in H, \tag{2.2}$$

where $\dot{u} \equiv \frac{\partial u}{\partial t}$, $h(\mu) \in H$ is the initial condition, and, as mentioned above, V is a Hilbert space appropriately chosen for the particular equation of interest. We assume that the parametrized linear form $f(\cdot;\cdot)$, bilinear form $a(\cdot,\cdot;\cdot)$, trilinear form $c(\cdot,\cdot,\cdot;\cdot)$, and initial condition $h(\cdot)$ are affine in functions of parameters and admit decompositions

$$f(v;\mu) = \sum_{q=1}^{Q^f} \Theta_q^f(\mu) f_q(v),$$
$$a(w,v;\mu) = \sum_{q=0}^{Q^a} \Theta_q^a(\mu) a_q(w,v),$$
$$c(w,z,v;\mu) = \sum_{q=1}^{Q^c} \Theta_q^c(\mu) c_q(w,z,v),$$
$$h(\mu) = \sum_{q=1}^{Q^h} \Theta_q^h(\mu) h_q,$$

where $f_q(\cdot)$, $q = 1,\dots,Q^f$, $a_q(\cdot,\cdot)$, $q = 0,\dots Q^a$, and $c_q(\cdot,\cdot,\cdot)$, $q = 1,\dots,Q^c$, are parameter-independent forms, $h_q \in H$, $q = 1,\dots,Q^h$, are parameter-independent functions, and Θ_q^f, Θ_q^a, Θ_q^c, and Θ_q^h are parameter-dependent functions that map from $\mathcal{D}$ to $\mathbb{R}$. We assume that $a_0(\cdot,\cdot)$ is symmetric and positive and defines a natural inner product and norm for the space V according to

$$(w,v)_V \equiv a_0(w,v) \quad \text{and} \quad \|w\|_V \equiv \sqrt{(w,w)_V}.$$

Furthermore, we assume that each of the trilinear forms is symmetric in the first two arguments

$$c_q(w,z,v) = c_q(z,w,v), \quad \forall w,z,v \in V, \quad q = 1,\dots,Q^c,$$

and is bounded in the sense that

$$c_q(w,z,v) \le C^{c_q} \|w\|_{L^4(\Omega)} \|z\|_{L^4(\Omega)} \|v\|_V, \quad \forall w,z,v \in V, \quad q = 1,\dots,Q^c, \tag{2.3}$$

for some constants C^{c_q}, $q = 1,\dots,Q^c$. For the inequality to be meaningful, we assume that $\|w\|_{L^4(\Omega)} \le \rho_{L^4(\Omega)\text{-}V} \|w\|_V$, $\forall w \in V$, for some Sobolev embedding constant $\rho_{L^4(\Omega)\text{-}V}$. Note that, for many governing equations of fluid flows, we may associate the diffusion term (positive and symmetric) with $a_0(\cdot,\cdot)$ and the convection term (written in a symmetrized form) with $c_1(\cdot,\cdot,\cdot)$.

2.2. Space-Time Variational Formulation. We now define Bochner spaces used in our space-time formulation. The $L^2(I;V)$ space is equipped with an inner product $(w,v)_{L^2(I;V)} \equiv \int_I (w(t),v(t))_V dt$ and the induced norm $\|w\|_{L^2(I;V)} \equiv \sqrt{(w,w)_{L^2(I;V)}}$. Its dual, $L^2(I;V')$, is equipped with an inner product $(w,v)_{L^2(I;V')} \equiv \int_I (Rw(t),Rv(t))_V dt$ and the induced norm $\|w\|_{L^2(I;V')} \equiv \sqrt{(w,w)_{L^2(I;V')}}$, where $R : V' \to V$ is the aforementioned Riesz operator on (V,H,V'). Finally, the space $H^1(I;V')$ is equipped with a (semi) inner product $(w,v)_{H^1(I;V')} \equiv (\dot{w},\dot{v})_{L^2(I;V')}$ and a (semi) norm $\|w\|_{H^1(I;V')} \equiv \sqrt{(w,w)_{H^1(I;V')}}$.

In order to treat nonzero initial conditions in a variational manner, we choose our space-time trial and test spaces following the work of Schwab and Stevenson [22]. The space-time trial space is given by

$$\mathcal{X} = L^2(I;V) \cap H^1(I;V')$$

and is equipped with an inner product

$$(w,v)_{\mathcal{X}} \equiv (w,v)_{H^1(I;V')} + (w,v)_{L^2(I;V)} + (w(T),v(T))_H \tag{2.4}$$

and the induced norm $\|w\|_{\mathcal{X}} \equiv \sqrt{(w,w)_{\mathcal{X}}}$. Note that $\mathcal{X}$ is not restricted to functions that vanish at $t = 0$. The norm is not the graph norm but includes the control of the solution at the final time as used by Urban and Patera [25]. Our space-time test space $\mathcal{Y}$ is

$$\mathcal{Y} = L^2(I;V) \times H$$

equipped with an inner product

$$(w,v)_{\mathcal{Y}} \equiv (w^{(1)},v^{(1)})_{L^2(I;V)} + (w^{(2)},v^{(2)})_H \tag{2.5}$$

and the induced norm $\|w\|_{\mathcal{Y}} = \sqrt{(w,w)_{\mathcal{Y}}}$ for $w \equiv (w^{(1)},w^{(2)})$ and $v \equiv (v^{(1)},v^{(2)})$. The second part of the couple, which is in H, is used to enforce the initial condition in a weak manner.

Our space-time semilinear form $\mathcal{G}(\cdot,\cdot;\mu) : \mathcal{X} \times \mathcal{Y} \to \mathbb{R}$ is given by

$$\begin{aligned}\mathcal{G}(w,v;\mu) = \dot{\mathcal{M}}(w,v^{(1)}) + \mathcal{A}(w,v^{(1)};\mu) + \mathcal{C}(w,w,v^{(1)};\mu) + \mathcal{F}(v;\mu) \\ + (w(0),v^{(2)})_H, \quad \forall w \in \mathcal{X},\ \forall v \in \mathcal{Y},\end{aligned}$$

where the parametrized space-time forms are given by integrating corresponding space-only forms with respect to time. Each space-time form inherits from its space-

only counterpart the operator decomposition that is affine in functions of parameters:

$$\begin{aligned}
\dot{\mathcal{M}}(w,v) &= \int_I \langle \dot{w}, v\rangle_{V'\times V} dt, \\
\mathcal{A}(w,v;\mu) &= \int_I a(w,v;\mu)dt = \sum_{q=0}^{Q^a} \Theta_q^a(\mu) \int_I a_q(w,v)dt \equiv \sum_{q=0}^{Q^a} \Theta_q^a(\mu)\mathcal{A}_q(w,v), \\
\mathcal{C}(w,z,v;\mu) &= \int_I c(w,z,v;\mu)dt = \sum_{q=1}^{Q^c} \Theta_q^c(\mu) \int_I c_q(w,z,v)dt \equiv \sum_{q=1}^{Q^c} \Theta_q^c(\mu)\mathcal{C}_q(w,z,v),
\end{aligned} \tag{2.6}$$

$$\begin{aligned}
\mathcal{F}(v;\mu) &= \int_I -f(v^{(1)};\mu)dt + (-h(\mu), v^{(2)})_H \\
&= \sum_{q=1}^{Q^f} \Theta_q^f(\mu) \int_I -f_q(v^{(1)})dt + \sum_{q=1}^{Q^h} \Theta_q^h(\mu)(-h_q, v^{(2)})_H \equiv \sum_{q=1}^{Q^{\tilde{f}}} \Theta_q^f(\mu)\mathcal{F}_q(v),
\end{aligned} \tag{2.7}$$

where $Q^{\tilde{f}} = Q^f + Q^h$; for notational convenience, we group the data terms that arise from the volume forcing f and the initial condition h into a single space-time functional $\mathcal{F}$. The space-time trilinear forms $\mathcal{C}_q(\cdot,\cdot,\cdot)$, $q = 1,\cdots,Q^c$, inherit the symmetry with respect to the first two arguments and the boundedness, i.e.

$$\begin{aligned}
&\mathcal{C}_q(w,z,v) = \mathcal{C}_q(z,w,v), \quad \forall w,z\in\mathcal{X},\ \forall v\in L^2(I;V),\ q=1,\dots,Q^c, \\
&\mathcal{C}_q(w,z,v) \le C^{c_q}\|w\|_{L^4(I;L^4(\Omega))}\|z\|_{L^4(I;L^4(\Omega))}\|v\|_{L^2(I;V)}, \\
&\qquad\qquad \forall w,z\in\mathcal{X},\ \forall v\in L^2(I;V),\ q=1,\dots,Q^c,
\end{aligned} \tag{2.8}$$

where C^{c_q}, $q = 1,\dots,Q^c$ are the constants in Eq. (2.3). The boundedness of the space-time trilinear form follows from integrating the inequality Eq. (2.3) in time and then twice invoking the Cauchy-Schwarz inequality. Note that for the bound to be useful, we have *assumed* that $\|w\|_{L^4(I;L^4(\Omega))} \le \rho_{L^4\text{-}\mathcal{X}}\|w\|_{\mathcal{X}}$, $\forall w\in\mathcal{X}$, for some Sobolev embedding constant $\rho_{L^4\text{-}\mathcal{X}}$; we will later verify this assumption for our discrete spaces.

Our space-time variational formulation yields the following weak statement: find $u(\mu)\in\mathcal{X}$ such that

$$\mathcal{G}(u(\mu),v;\mu) = 0, \quad \forall v\in\mathcal{Y}.$$

The Fréchet derivative bilinear form associated with $\mathcal{G}$ evaluated about $z\in\mathcal{X}$ is denoted by $\partial\mathcal{G}(\cdot,z,\cdot;\cdot)$ and is given by

$$\partial\mathcal{G}(w,z,v;\mu) = \dot{\mathcal{M}}(w,v) + \mathcal{A}(w,v;\mu) + 2\mathcal{C}(w,z,v;\mu)\ ;$$

the linearization of $\mathcal{C}$ follows from its symmetry with respect to the first two arguments.

2.3. Finite Element Discretization. We consider the standard Galerkin discretization in space and a discontinuous Galerkin (DG) discretization in time [15, 10]. Let us denote our spatial finite element space by V_h, where the subscript h signifies the characteristic diameter of elements in the triangulation $\mathcal{T}_h$ of the domain Ω. The choice of the spatial finite element is dependent on the particular equation of interest;

for example, the standard linear finite element may be used for Burgers' equation, whereas Taylor-Hood finite element would be better suited for the incompressible Navier-Stokes equations.

For our temporal discretization, we first partition the interval $I \equiv (0,T]$ into K non-overlapping intervals $I^k = (t^{k-1}, t^k]$, $k = 1, \ldots, K$, delineated by $0 = t^0 < t^1 < \cdots < t^K = T$. Our DG temporal finite element space is given by

$$S_{\Delta t} = \{v \in L^2(I) : v|_{I^k} \in \mathbb{P}^p(I^k), k = 1, \ldots, K\},$$

where $\mathbb{P}^p(I^k)$ denotes the space of degree-p univariate polynomials on the interval I^k. Our temporal finite element space is non-conforming and discontinuous in time.

We denote our space-time finite element trial and test spaces by

$$\mathcal{X}_\delta = S_{\Delta t} \otimes V_h \quad \text{and} \quad \mathcal{Y}_\delta = S_{\Delta t} \otimes V_h,$$

respectively. The subscript $\delta \equiv (\Delta t, h)$ signifies that the spaces are dependent on both the temporal and spatial meshes; we denote the dimension of the space-time finite element spaces by $\mathcal{N}$, i.e., $\mathcal{N} \equiv \dim(\mathcal{X}_\delta) = \dim(\mathcal{Y}_\delta)$. Note that unlike its continuous counterpart, our choice of the $\mathcal{Y}_\delta$ space is *not* a couple of functions over $\Omega \times I$ and Ω, the latter of which is used to enforce the initial condition.

To facilitate the presentation of norms associated with our finite element space, let us first recall the DG discretization of the temporal evolution bilinear form $\dot{\mathcal{M}}(\cdot,\cdot)$. The DG discretization for the evolution term is given by

$$\dot{\mathcal{M}}_\delta(w,v) \equiv \sum_{k=1}^{K} \int_{I^k} \langle \dot{w}, v \rangle_{V' \times V} dt + \sum_{k=2}^{K} \left(w(t_+^{k-1}) - w(t_-^{k-1}), v(t_+^{k-1}) \right)_H ,$$

where $w(t_+^k) \equiv \lim_{\epsilon \to 0^+} w(t^k + \epsilon)$ and $w(t_-^k) \equiv \lim_{\epsilon \to 0^+} w(t^k - \epsilon)$ are based on the function values in interval I^{k+1} and I^k, respectively [10].

We equip our space-time finite element test space $\mathcal{Y}_\delta$ with a discrete analog of the $\mathcal{Y}$ inner product Eq. (2.5),

$$(w,v)_{\mathcal{Y}_\delta} \equiv (w,v)_{L^2(I;V)} + (w(t_+^0), v(t_+^0))_H,$$

and the induced norm $\|v\|_{\mathcal{Y}_\delta} \equiv \sqrt{(v,v)_{\mathcal{Y}_\delta}}$. Note that the $\mathcal{Y}_\delta$ inner product is decoupled in time owing to the time-discontinuous test functions. The trial space $\mathcal{X}_\delta$, on the other hand, is equipped with an inner product

$$\begin{aligned}(w,v)_{\mathcal{X}_\delta} \equiv (R_\delta w, R_\delta v)_{\mathcal{Y}_\delta} + (w,v)_{L^2(I;V)} + (w(t_-^K), w(t_-^K))_H \\ + \sum_{k=2}^{K} \left(w(t_+^{k-1}) - w(t_-^{k-1}), v(t_+^{k-1}) - v(t_-^{k-1}) \right)_H ,\end{aligned}$$

where the lifting operator $R_\delta : \mathcal{X}_\delta \to \mathcal{Y}_\delta$ satisfies, for each $w \in \mathcal{X}_\delta$,

$$(R_\delta w, v)_{\mathcal{Y}_\delta} = \dot{\mathcal{M}}_\delta(w,v), \quad \forall v \in \mathcal{Y}_\delta \ ; \tag{2.9}$$

the associated induced norm is $\|w\|_{\mathcal{X}_\delta} \equiv \sqrt{(w,w)_{\mathcal{X}_\delta}}$. We choose our lifting operator in a manner that is consistent with the DG interpretation of the temporal derivative operator, which includes the jump contribution. In addition, our $\mathcal{X}_\delta$ norm includes the extra jump penalty term. As we will see shortly, this choice of the $\mathcal{X}_\delta$ norm in fact

arises naturally when we consider the DG discretization of the heat equation. The $\mathcal{X}_\delta$ inner product is coupled in time through the jump terms in the lifting term and the penalty term.

The combination of the DG temporal scheme and spatial finite element discretization yields our space-time finite element statement: find $u_\delta(\mu) \in \mathcal{X}_\delta$ such that

$$\mathcal{G}_\delta(u_\delta(\mu), v; \mu) = 0, \quad \forall v \in \mathcal{Y}_\delta, \tag{2.10}$$

where the discrete semilinear form is give by

$$\mathcal{G}_\delta(w, v; \mu) \equiv \dot{\mathcal{M}}_\delta(w, v) + \mathcal{A}(w, v; \mu) + \mathcal{C}(w, w, v; \mu) + \mathcal{F}_\delta(v; \mu) + (w(t_+^0), v(t_+^0))_H \ ;$$

here, the data term, which includes the initial condition, is given by

$$\mathcal{F}_\delta(v; \mu) = \int_I -f(v; \mu)dt + (-h(\mu), v(t_+^0))_H \ .$$

The well-posedness of the finite element formulation will be verified *a posteriori* by the Brezzi-Rappaz-Raviart theory. The Fréchet derivative associated with $\mathcal{G}_\delta$ evaluated about $z \in \mathcal{X}_\delta$ is denoted by $\partial\mathcal{G}_\delta$ and is given by

$$\partial\mathcal{G}_\delta(w, z, v; \mu) \equiv \dot{\mathcal{M}}_\delta(w, v) + \mathcal{A}(w, v; \mu) + 2\mathcal{C}(w, z, v; \mu) + (w(t_+^0), v(t_+^0))_H,$$

where we again appeal to the symmetry of $\mathcal{C}$ in the first two arguments.

With the above space-time discretization and (discrete) norms, we have the following statement for the heat equation[4]:

THEOREM 2.1. *For the heat equation, which is defined by the semilinear form*

$$\mathcal{G}_\delta^{\text{heat}}(w, v) \equiv \dot{\mathcal{M}}_\delta(w, v) + \mathcal{A}_0(w, v) + (w(t_+^0), v(t_+^0)) + \mathcal{F}_\delta(v),$$

the inf-sup constant is

$$\beta^{\text{heat}} \equiv \inf_{w \in \mathcal{X}_\delta} \sup_{v \in \mathcal{Y}_\delta} \frac{\partial\mathcal{G}_\delta^{\text{heat}}(w, v)}{\|w\|_{\mathcal{X}_\delta} \|v\|_{\mathcal{Y}_\delta}} = 1,$$

and the continuity constant is

$$\gamma^{\text{heat}} \equiv \sup_{w \in \mathcal{X}_\delta} \sup_{v \in \mathcal{Y}_\delta} \frac{\partial\mathcal{G}_\delta^{\text{heat}}(w, v)}{\|w\|_{\mathcal{X}_\delta} \|v\|_{\mathcal{Y}_\delta}} = 1,$$

where $\partial\mathcal{G}_\delta^{\text{heat}}(w, v) \equiv \mathcal{M}_\delta(w, v) + \mathcal{A}_0(w, v) + (w(t_+^0), v(t_+^0))_H$.

Proof. First, because $a_0(w, v) = (w, v)_V$, we have $A_0(w, v) = (w, v)_{L^2(I;V)}$. Thus, our Fréchet derivative bilinear form is given by

$$\begin{aligned}
\partial\mathcal{G}_\delta^{\text{heat}}(w, v) &= \dot{\mathcal{M}}_\delta(w, v) + \mathcal{A}_0(w, v) + (w(t_+^0), v(t_+^0))_H \\
&= \dot{\mathcal{M}}_\delta(w, v) + (w, v)_{L^2(I;V)} + (w(t_+^0), v(t_+^0))_H \\
&= \dot{\mathcal{M}}_\delta(w, v) + (w, v)_{\mathcal{Y}_\delta},
\end{aligned}$$

where the last equality follows from the definition of the $\mathcal{Y}_\delta$ inner product. Let us introduce a supremizing operator $S : \mathcal{X}_\delta \to \mathcal{Y}_\delta$ associated with the bilinear form,

$$(Sw, v)_{\mathcal{Y}_\delta} = \partial\mathcal{G}_\delta^{\text{heat}}(w, v), \quad \forall w \in \mathcal{X}_\delta, \ v \in \mathcal{Y}_\delta.$$

[4]In the context of Navier-Stokes equation, the "heat equation" corresponds to the Stokes equations.

Because $\partial\mathcal{G}_\delta^{\text{heat}}(w,v) = \dot{\mathcal{M}}_\delta(w,v) + (w,v)_{\mathcal{Y}_\delta}$, the supremizing operator may be decomposed as $S = S^{\dot{\mathcal{M}}} + Id$ where

$$(S^{\dot{\mathcal{M}}}w, v)_{\mathcal{Y}_\delta} = \dot{\mathcal{M}}_\delta(w,v), \quad \forall w \in \mathcal{X}_\delta,\ v \in \mathcal{Y}_\delta.$$

We recognize $S^{\dot{\mathcal{M}}} = R_\delta$, where R_δ is the DG lifting operator defined by Eq. (2.9). We then substitute the definition of the supremizing operator to the expression for the inf-sup constant and the continuity constant and solve the supremization problem on $\mathcal{Y}_\delta$ using the Cauchy-Schwarz inequality (which yields $v_{\text{sup}} = Sw$) to obtain

$$\beta^{\text{heat}} = \inf_{w\in\mathcal{X}_\delta} \frac{\|Sw\|_{\mathcal{Y}_\delta}}{\|w\|_{\mathcal{X}_\delta}} \quad \text{and} \quad \gamma^{\text{heat}} = \sup_{w\in\mathcal{X}_\delta} \frac{\|Sw\|_{\mathcal{Y}_\delta}}{\|w\|_{\mathcal{X}_\delta}}. \tag{2.11}$$

Using the decomposition for our supremizing operator, $S = R_\delta + Id$, the (square of the) numerator of Eq. (2.11) can be expressed as

$$\|Sw\|_{\mathcal{Y}_\delta}^2 = (R_\delta w, R_\delta w)_{\mathcal{Y}_\delta} + (w,w)_{\mathcal{Y}_\delta} + 2(R_\delta w, w)_{\mathcal{Y}_\delta}.$$

We now appeal to the definition of the lifting operator R_δ, invoke integration by parts to (the half of) $\langle \dot{w}, w\rangle_{V'\times V}$, and carry out algebraic manipulation to simplify the last term of the right-hand side:

$$(R_\delta w, w)_{\mathcal{Y}_\delta} = \dot{\mathcal{M}}_\delta(w,w) = \sum_{k=1}^K \int_{I^k} \langle \dot{w}, w\rangle_{V'\times V} dt + \sum_{k=2}^K \left(w(t_+^{k-1}) - w(t_-^{k-1}), w(t_+^{k-1})\right)_H$$

$$= \frac{1}{2}\left[-\|w(t_+^0)\|_H^2 + \sum_{k=2}^K \|w(t_+^{k-1}) - w(t_-^{k-1})\|_H^2 + \|w(t_-^K)\|_H^2\right].$$

Thus, the numerator of Eq. (2.11) simplifies to

$$\|Sw\|_{\mathcal{Y}_\delta}^2 = (R_\delta w, R_\delta w)_{\mathcal{Y}_\delta} + (w,w)_{\mathcal{Y}_\delta} - \|w(t_+^0)\|_H^2 + \sum_{k=1}^{K-1} \|w(t_+^k) - w(t_-^k)\|_H^2 + \|w(t_-^K)\|_H^2$$

$$= (R_\delta w, R_\delta w)_{\mathcal{Y}_\delta} + (w,w)_{L^2(I;V)} + \|w(t_-^K)\|_H^2 + \sum_{k=1}^{K-1} \|w(t_+^k) - w(t_-^k)\|_H^2.$$

This is precisely our definition of the $\mathcal{X}_\delta$ norm. Thus, we have $\|Sw\|_{\mathcal{Y}_\delta}/\|w\|_{\mathcal{X}_\delta} = 1$, $\forall w \in \mathcal{X}_\delta$, which proves the desired results. □

Remark 2.2. The above proof shows that our $\mathcal{X}_\delta$ norm (and inner product), which is closely related to the graph norm of $H^1(I;V') \times L^2(I;V)$, is in fact the (space-time) natural norm (and inner product) [23] associated with the DG discretization of the heat equation with the $\mathcal{Y}_\delta$ test norm. In Section 3.5, we will take advantage of this equivalence to efficiently solve the $\mathcal{X}_\delta$-projection problem.

Remark 2.3. Our space-time DG discretization for piecewise constant ($p = 0$) temporal approximation space is equivalent to the backward Euler discretization of the parabolic equation (see, e.g. Eriksson and Johnson [10]). Thus, the space-time DG finite element formulation and associated space-time norms yield a variational framework for the backward Euler scheme.

Let us make a few comments on the computational cost associated with the solution of the DG-in-time system, Eq. (2.10). Due to the time-discontinuous nature of the DG temporal discretization, Eq. (2.10) can be solved one time interval at a time, starting from I^1. Each time step requires the solution of a $(p+1)\cdot\dim(V_h)$-dimensional nonlinear equation, which is solved using the Newton's method. Note that, to achieve second-order accuracy using the DG discretization, we must solve a system that is twice as large as the Crank-Nicolson system at each time step; however, we accept the additional cost for the L- and algebraic stability of the DG formulation [2].

The use of DG-in-time discretization instead of the Crank-Nicolson time-stepping — as considered in the preceding papers [25, 28] — is motivated by its better stability properties; in particular, the (discrete) L^4-$\mathcal{X}_\delta$ Sobolev embedding constant depends only weakly on the temporal and spatial meshes, as we will demonstrate in Section 3.5. (Note that the DG discretization also enables arbitrarily high-order discretization by increasing the polynomial order — the property often noted by its practitioners; however, our primary interest here is its stability and variational construction, which facilitate the error analysis.)

3. Space-Time Certified Reduced Basis Method. Our space-time certified reduced basis method is based on the *hp* reduced basis method of Eftang *et al.* [9] In the *hp* reduced basis method, the parameter space $\mathcal{D} \subset \mathbb{R}^P$ is partitioned into N_μ non-overlapping subdomains $\mathcal{D}_j$, $j = 1, \ldots, N_\mu$. For each subdomain $\mathcal{D}_j$, we associate reduced basis approximation space $\mathcal{X}_{N_j,\mathcal{D}_j} \subset \mathcal{X}_\delta$ of dimension N_j. In this section, we construct our space-time reduced basis approximation and associated error bounds for single partition *assuming that the partitions $\mathcal{D}_j$ and the trial space $\mathcal{X}_{N_j,\mathcal{D}_j}$ have already been constructed.* We detail the selection of the partition and spaces in Section 4. In addition, to avoid notational clutter — and as the focus of this section is approximation and certification for a *single* partition, we will simply denote the trial space associated with the partition of interest by $\mathcal{X}_N$ instead of $\mathcal{X}_{N_j,\mathcal{D}_j}$, where the subscript N signifies the dimension of the particular reduced basis space.

3.1. Space-Time Petrov-Galerkin Reduced Basis Approximation. Because our space-time semilinear form is non-coercive, the standard Galerkin projection is not guaranteed to yield a good — or even a stable — approximation. Thus, we employ the minimum residual formulation of Maday *et al.* [18] for our space-time reduced basis approximation. First, note that the dual norm of the residual may be expressed as

$$\|\mathcal{G}_\delta(w_N,\ \cdot\ ;\mu)\|_{\mathcal{Y}_\delta'} = \sup_{v\in\mathcal{Y}_\delta} \frac{\mathcal{G}_\delta(w_N, v;\mu)}{\|v\|_{\mathcal{Y}_\delta}} = \|\mathcal{S}(w_N;\mu)\|_{\mathcal{Y}_\delta}\ ,$$

where $\mathcal{S}(w_N;\mu) \in \mathcal{Y}_\delta$ satisfies

$$(\mathcal{S}(w_N;\mu), v)_{\mathcal{Y}_\delta} = \mathcal{G}_\delta(w_N, v;\mu), \quad \forall v \in \mathcal{Y}_\delta\ .$$

Then, given a reduced basis trial space $\mathcal{X}_N \subset \mathcal{X}_\delta$, we seek $u_N(\mu) \in \mathcal{X}_N$ such that

$$\begin{aligned} u_N(\mu) &= \arg\inf_{w_N\in\mathcal{X}_N} \|\mathcal{G}_\delta(w_N,\ \cdot\ ;\mu)\|_{\mathcal{Y}_\delta'} = \arg\inf_{w_N\in\mathcal{X}_N} \sup_{v\in\mathcal{Y}_\delta} \frac{\mathcal{G}_\delta(w_N, v;\mu)}{\|v\|_{\mathcal{Y}_\delta}} \\ &= \arg\inf_{w_N\in\mathcal{X}_N} \|\mathcal{S}(w_N;\mu)\|_{\mathcal{Y}_\delta}\ . \end{aligned} \tag{3.1}$$

We remark on the optimality of the approximation in a certain sense:

Remark 3.1. The minimum residual scheme may be interpreted as a Petrov-Galerkin projection with the stability-maximizing test space. To see this, note that the first-order optimality condition associated with the minimization statement Eq. (3.1) is

$$(\mathcal{S}(w_N;\mu),\mathcal{S}'[w_N](z_N;\mu))_{\mathcal{Y}_\delta} = 0, \quad \forall z_N \in \mathcal{X}_N, \tag{3.2}$$

where the derivative operator satisfies

$$(\mathcal{S}'[w_N](z_N;\mu),v)_{\mathcal{Y}_\delta} = \partial\mathcal{G}_\delta(z_N,w_N,v;\mu), \quad \forall v \in \mathcal{Y}_\delta \ .$$

Then, by the definition of the supremizing operator, we have

$$\mathcal{G}_\delta(u_N(\mu),\mathcal{S}'[u_N(\mu)](z_N;\mu);\mu) = 0, \quad \forall z_N \in \mathcal{X}_N \ ,$$

or, equivalently, by appealing to the definition of $\mathcal{S}'[u_N(\mu)](z_N;\mu)$,

$$\mathcal{G}_\delta(u_N(\mu),v_N;\mu) = 0, \quad \forall v_N \in \mathcal{Y}_N(\mathcal{X}_N;u_N(\mu),\mu),$$

where

$$\mathcal{Y}_N(\mathcal{X}_N;u_N(\mu),\mu) = \left\{ v \in \mathcal{Y}_\delta : v = \arg\sup_{v' \in \mathcal{Y}_\delta} \frac{\partial\mathcal{G}_\delta(w,u_N(\mu),v';\mu)}{\|w\|_{\mathcal{X}_\delta}\|v'\|_{\mathcal{Y}_\delta}}, w \in \mathcal{X}_N \right\} \ .$$

Note that $\mathcal{Y}_N(\mathcal{X}_N;u_N(\mu),\mu) \subset \mathcal{Y}_\delta$ is the space of the inf-sup supremizers of the Fréchet derivative bilinear form linearized about u_N associated with the space $\mathcal{X}_N$. Consequently, the inf-sup constant of the Petrov-Galerkin reduced basis problem is bounded below by that of the finite element problem. In particular, the reduced basis problem is well-posed given the finite element problem is well-posed. (For a similar stability-guaranteed formulation for the Brezzi inf-sup condition (rather than the Babuška inf-sup condition used here), see Rozza and Veroy [21].)

We now demonstrate that the solution of Eq. (3.1) permits *offline-online* computational decomposition. Given a $\mathcal{X}_\delta$-orthonormalized set of space-time trial-space basis functions, $\{\xi_k\}_{k=1}^N$, we wish to find $\alpha_N(\mu) \in \mathbb{R}^N$ such that $u_N(\mu) = \xi_k\alpha_{Nk}(\mu)$. Appealing to the affine decomposition of our semilinear form, we can express our supremizer $\mathcal{S}(w_N;\mu)$ as

$$\mathcal{S}(w_N;\mu) = \chi_k^{\dot{\mathcal{M}}}\alpha_{Nk} + \Theta_q^a(\mu)\chi_k^{\mathcal{A}_q}\alpha_{Nk} + \Theta_q^c(\mu)\chi_{kl}^{\mathcal{C}_q}\alpha_{Nk}\alpha_{Nl} + \Theta_q^f(\mu)\chi^{\mathcal{F}_q},$$

where the basis functions for the supremizer is the Riesz representations of our parameter-independent space-time forms:

$$\begin{aligned}
(\chi_k^{\dot{\mathcal{M}}},v)_{\mathcal{Y}_\delta} &= \dot{\mathcal{M}}(\xi_k,v), \quad \forall v \in \mathcal{Y}_\delta,\ k = 1,\dots,N,\\
(\chi_k^{\mathcal{A}_q},v)_{\mathcal{Y}_\delta} &= \mathcal{A}_q(\xi_k,v), \quad \forall v \in \mathcal{Y}_\delta,\ k = 1,\dots,N,\ q = 0,\dots,Q^a,\\
(\chi_{kl}^{\mathcal{C}_q},v)_{\mathcal{Y}_\delta} &= \mathcal{C}_q(\xi_k,\xi_l,v), \quad \forall v \in \mathcal{Y}_\delta,\ k,l = 1,\dots,N,\ q = 1,\dots,Q^c,\\
(\chi^{\mathcal{F}_q},v)_{\mathcal{Y}_\delta} &= \mathcal{F}_q(v), \quad \forall v \in \mathcal{Y}_\delta,\ q = 1,\dots,Q^{\tilde{f}} \ .
\end{aligned} \tag{3.3}$$

The supremizer $\mathcal{S}(w_N;\mu)$ is expressed as a linear combination of $N+Q^aN+\frac{1}{2}Q^cN(N+1)+Q^{\tilde{f}}$ parameter-independent basis functions. The (square of the) dual norm of the

residual is then expressed as

$$
\begin{aligned}
&\|\mathcal{S}(\xi_k\alpha_k;\mu)\|^2_{\mathcal{Y}_\delta} \\
&= (\chi_k^{\dot{\mathcal{M}}},\chi_i^{\dot{\mathcal{M}}})_{\mathcal{Y}_\delta}\alpha_k\alpha_i + 2\Theta_p^a(\mu)(\chi_k^{\dot{\mathcal{M}}},\chi_i^{\mathcal{A}_p})_{\mathcal{Y}_\delta}\alpha_k\alpha_i + 2\Theta_p^c(\mu)(\chi_k^{\dot{\mathcal{M}}},\chi_{ij}^{\mathcal{C}_p})_{\mathcal{Y}_\delta}\alpha_k\alpha_i\alpha_j \\
&\quad + 2\Theta_p^f(\mu)(\chi_k^{\dot{\mathcal{M}}},\chi^{\mathcal{F}_p})_{\mathcal{Y}_\delta}\alpha_k + \Theta_q^a(\mu)\Theta_p^a(\mu)(\chi_k^{\mathcal{A}_q},\chi_k^{\mathcal{A}_p})_{\mathcal{Y}_\delta}\alpha_k\alpha_i \\
&\quad + 2\Theta_q^a(\mu)\Theta_p^c(\mu)(\chi_k^{\mathcal{A}_q},\chi_{ij}^{\mathcal{C}_p})_{\mathcal{Y}_\delta}\alpha_k\alpha_i\alpha_j + 2\Theta_q^a(\mu)\Theta_p^f(\mu)(\chi_k^{\mathcal{A}_q},\chi^{\mathcal{F}_p})_{\mathcal{Y}_\delta}\alpha_k \\
&\quad + \Theta_q^c(\mu)\Theta_p^c(\mu)(\chi_{kl}^{\mathcal{C}_q},\chi_{ij}^{\mathcal{C}_p})_{\mathcal{Y}_\delta}\alpha_k\alpha_l\alpha_i\alpha_j + 2\Theta_q^c(\mu)\Theta_p^f(\mu)(\chi_{kl}^{\mathcal{C}_q},\chi^{\mathcal{F}_p})_{\mathcal{Y}_\delta}\alpha_k\alpha_l \\
&\quad + \Theta_q^f(\mu)\Theta_p^f(\mu)(\chi^{\mathcal{F}_q},\chi^{\mathcal{F}_p})_{\mathcal{Y}_\delta}\ . \qquad (3.4)
\end{aligned}
$$

Tedious but straightforward differentiation of Eq. (3.4) yields the first order optimality condition for Eq. (3.1), which corresponds to Eq. (3.2). The differentiation of the optimality condition then yields the Hessian, which is used to solve the optimization problem using Newton's method.

The *offline-online* computational procedure is now clear from Eq. (3.4). In the *offline* stage, we first compute the Riesz representations $\chi_k^{\mathcal{M}}$, $\chi_k^{A_q}$, $\chi_{kl}^{\mathcal{C}_q}$, and $\chi^{\mathcal{F}_q}$ in $\mathcal{O}(\mathcal{N}\cdot(1+Q^aN+Q^cN^2+Q^{\tilde{f}}))$ operations. We then compute the inner products of Riesz representations that appear in Eq. (3.4). In the *online* stage, we assemble the reduced basis residual (and the associated derivative and Hessian) using Eq. (3.4) in $\mathcal{O}((Q^c)^2N^4)$ operations and solve the nonlinear problem using Newton's method. In particular, the online cost is independent of the finite element complexity $\mathcal{N}$, which includes the number of time steps K (c.f. time-marching POD-based approach of, e.g., Haasdonk and Ohlberger [13]).

Remark 3.2. In practice, for many problems we have considered, the standard Galerkin projection works well. However, the Galerkin formulation is theoretically less sound, i.e. unproven stability. As the size of reduced basis system is small — especially in the space-time *and hp* context, we prefer the minimum residual (or Petrov-Galerkin) formulation presented above.

3.2. Brezzi-Rappaz-Raviart Error Bound. As in our previous work on Burgers' equation [28], our space-time *a posteriori* error bound relies on the Brezzi-Rappaz-Raviart (BRR) theory:

THEOREM 3.3. *Let $\tau_N(\mu)$ be a normalized residual associated with an approximation $u_N(\mu)$ defined by*

$$\tau_N(\mu) \equiv \frac{4\gamma^2(\mu)}{(\beta_N^{LB}(\mu))^2}\epsilon_N(\mu), \qquad (3.5)$$

where the continuity constant of the trilinear form, $\gamma(\mu)$, a lower bound of inf-sup constant of the linearized form, $\beta_N^{LB}(\mu)$, and the dual norm of the residual, $\epsilon_N(\mu)$, satisfy, respectively,

$$
\begin{aligned}
\mathcal{C}(w,z,v;\mu) &\le \gamma^2(\mu)\|w\|_{\mathcal{X}_\delta}\|z\|_{\mathcal{X}_\delta}\|v\|_{\mathcal{Y}_\delta} \\
\beta_N^{LB}(\mu) \le \beta_N &\equiv \inf_{w\in\mathcal{X}_\delta}\sup_{v\in\mathcal{Y}_\delta}\frac{\partial\mathcal{G}(w,u_N(\mu),v;\mu)}{\|w\|_{\mathcal{X}_\delta}\|v\|_{\mathcal{Y}_\delta}} \qquad (3.6) \\
\epsilon_N(\mu) &\equiv \|\mathcal{G}(u_N,\cdot\,;\mu)\|_{\mathcal{Y}_\delta'} = \sup_{v\in\mathcal{Y}_\delta}\frac{\mathcal{G}(u_N(\mu),v;\mu)}{\|v\|_{\mathcal{Y}_\delta}}\ . \qquad (3.7)
\end{aligned}
$$

Suppose the normalized residual is less than unity:

$$\tau_N(\mu) < 1\,. \qquad (3.8)$$

Then, there exists a unique solution $u_\delta(\mu) \in \mathfrak{B}(u_N(\mu), \beta_N^{LB}(\mu)/(2\gamma^2(\mu)))$ *to Eq.* (2.10) *where* $\mathfrak{B}(z,r) \equiv \{w \in \mathcal{X}_\delta : \|w - z\|_{\mathcal{X}_\delta} < r\}$. *Moreover, the error in* $u_N(\mu)$ *is bounded by*

$$\|u_\delta(\mu) - u_N(\mu)\|_{\mathcal{X}_\delta} \leq \Delta_N(\mu) \equiv \frac{\beta_N^{LB}(\mu)}{2\gamma^2(\mu)} \left(1 - \sqrt{1 - \tau_N(\mu)}\right) . \tag{3.9}$$

Proof. The proof for quadratic nonlinearity is provided in, e.g., Veroy and Patera [26]. □

Remark 3.4. For a trilinear form Eq. (2.7) with the parameter-independent forms bounded in the sense of Eq. (2.8), the continuity constant γ^2 is given by

$$\gamma^2(\mu) = \rho^2 \Theta_q^c(\mu) C^{c_q},$$

where C^{c_q}, $q = 1, \ldots, Q^c$, are the continuity constants in Eq. (2.3), and ρ is the space-time L^4-$\mathcal{X}_\delta$ Sobolev embedding constant defined by

$$\rho \equiv \sup_{w \in \mathcal{X}_\delta} \frac{\|w\|_{L^4(I;L^4(\Omega))}}{\|w\|_{\mathcal{X}_\delta}}. \tag{3.10}$$

It can be shown [17] that, in two dimensions, the space-time L^4-$\mathcal{X}_\delta$ embedding constant is bounded independent of the mesh size δ; however, in three dimensions, the constant is weakly dependent on the mesh size. We will study the behavior of the constant and provide associated computational techniques in Section 3.5.

Remark 3.5. The condition Eq. (3.8) defines a neighborhood of the solution $u_N(\mu)$ about which the effect of the quadratic term is rigorously bounded and hence the linear theory applies. In the limit of $\epsilon_N(\mu) \to 0$, the BRR bound reduces to a more familiar linear bound: $\Delta_N(\mu) \to \epsilon_N(\mu)/\beta_N^{\mathrm{LB}}(\mu)$; in addition, for any $\tau_N(\mu) < 1$, the BRR error bound is bounded from above by $\Delta_N(\mu) \leq 2\epsilon_N(\mu)/\beta_N^{\mathrm{LB}}(\mu)$.

Remark 3.6. The condition on the normalized residual Eq. (3.8) imposes a constraint on the maximum error level that can be certified using the BRR error bound procedure. Namely, if $\tau_N < 1$, then

$$\Delta_N < \frac{\beta_N^{\mathrm{LB}}(\mu)}{2\gamma^2(\mu)} = \frac{\beta_N^{\mathrm{LB}}(\mu)}{2\rho^2 \sum_{q=1}^{Q_c} \Theta_q^c(\mu) C^{c_q}} \equiv E \ . \tag{3.11}$$

In other words, we cannot certify — that is, cannot provide any error bound for — a low-fidelity reduced basis approximation whose error is greater than E even if we assume the perfect effectivity. This is unlike in the linear case, where error bounds may be constructed for reduced basis approximation of any fidelity.

The construction of our space-time error bound requires evaluation of the following quantities: 1) the dual norm of the residual defined by Eq. (3.7); 2) an inf-sup lower bound satisfying Eq. (3.6); and 3) the Sobolev embedding constant Eq. (3.10), which in turn provides a continuity constant γ. In the following three sections, we detail evaluation and approximation of these three quantities, with particular emphasis on *offline-online* computational decomposition.

3.3. Dual Norm of the Residual. In Section 3.1, we have already developed an explicit expression for the dual norm of the residual, $\epsilon_N(\mu) \equiv \|\mathcal{G}_\delta(w_N, \cdot\,; \mu)\|_{\mathcal{Y}_\delta'} = \|S(w_N; \mu)\|_{\mathcal{Y}_\delta}$, in Eq. (3.4). The standard offline-online computational decomposition appeals directly to Eq. (3.4) and evaluates the residual in online complexity independent of $\mathcal{N}$. However, this procedure is known to suffer from numerical precision issues

if high accuracy is desired [4]; the precision issue arise because the residual evaluation relies on cancellation of $\mathcal{O}(1)$ inner product pieces. A solution to this problem was recently proposed by Casenave [5]. Casenave's idea is based on representing the dual norm of the residual not as a linear combination of inner product pieces, each of which is of $\mathcal{O}(1)$, but as a linear combination of residuals evaluated at different parameter points, each of which is of order of the residual itself. Recently, Casenave has further improved the conditioning and computational efficiency of the procedure by incorporating the empirical interpolation method (EIM) [1] in his residual evaluation procedure [6]. We use this latter procedure to enable more round-off resistant *offline-online* computational decomposition of the residual dual norm evaluation.

First, we note that the (square of the) dual norm of the residual, as expressed in Eq. (3.4), can be interpreted as an inner product of two M-vectors, where M is the number of terms in Eq. (3.4): a parameter-independent vector $g \in \mathbb{R}^M$ whose entries consist of the inner products of the basis functions for the Riesz representation of the residual, e.g. $(\chi_k^{\dot{\mathcal{M}}}, \chi_m^{\dot{\mathcal{M}}})_{\mathcal{Y}_\delta}$, and a parameter-dependent vector $\theta(\mu) \in \mathbb{R}^M$ whose entries consist of the affine decomposition weights $\Theta(\mu)$ and reduced basis coefficients $\alpha(\mu)$. We thus have

$$\epsilon_N^2(\mu) = \sum_{k=1}^{M} g_k \theta_k(\mu). \tag{3.12}$$

To reduce the size of the problem, we now apply the EIM procedure to $\theta : \mathcal{D} \to \mathbb{R}^M$ and approximate it as a linear combination

$$\theta(\mu) \approx \sum_{j=1}^{M_{\text{EIM}}} \theta(\mu_j^*)\sigma_j(\mu),$$

where $M_{\text{EIM}} \leq M$ (formally but $M_{\text{EIM}} \ll M$ in practice) is the number of EIM interpolation points, and $\sigma(\mu)$ is selected to satisfy the interpolation condition

$$P_{i^*(i)}\theta_{i^*(i)}(\mu) = \sum_{j=1}^{M_{\text{EIM}}} P_{i^*(i)}\theta_{i^*(i)}(\mu_j^*)\sigma_j(\mu), \quad \text{(no sum on } i\text{)}, \qquad i = 1, \ldots, M_{\text{EIM}}. \tag{3.13}$$

Here, $\{\mu_j^*\}_{j=1}^{M_{\text{EIM}}}$ is a set of EIM parameter interpolation points and $\{i^*(i)\}_{i=1}^{M_{\text{EIM}}}$ is a set of EIM interpolation indices; both sets are chosen in a Greedy manner following the standard EIM procedure; see, e.g., Barrault *et al.* [1] The variable $P_{i^*(i)}$ is a simple preconditioner for the interpolation problem: $P_{i^*(i)} = (\sup_{\mu\in\Xi} \theta_{i^*(i)}(\mu))^{-1}$, $i = 1, \ldots, M_{\text{EIM}}$. With the EIM approximation, Eq. (3.12) becomes

$$\epsilon_N^2(\mu) \approx g_k \left(\theta_k(\mu_j^*)\sigma_j(\mu)\right) = \left(g_k\theta_k(\mu_j^*)\right)\sigma_j(\mu) = \epsilon_N^2(\mu_j^*)\sigma_j(\mu)\ . \tag{3.14}$$

The dual norm of the residual for a particular parameter is expressed as a linear combination of the dual norm of the residual at select M_{EIM} EIM interpolation points.

The *online-offline* computational decomposition of the EIM-based residual-norm approximation procedure is apparent from the construction. In the *offline* stage, we select the EIM interpolation parameters $\{\mu_j^*\}_{j=1}^{M_{\text{EIM}}}$ and indices $\{i^*(i)\}_{i=1}^{M_{\text{EIM}}}$, construct (the PLU factors of) the preconditioned EIM interpolation matrix $(P_{i^*(i)}\theta_{i*(i)}(\mu_j^*))_{i,j=1}^{M_{\text{EIM}}}$, and evaluate the residual vector $(\epsilon_N^2(\mu_j^*))_{j=1}^{M_{\text{EIM}}}$. In the *online* stage, we compute $(\theta_{i^*(i)}(\mu))_{i=1}^{M_{\text{EIM}}}$, solve the interpolation condition Eq. (3.13) for $\sigma(\mu)$, and evaluate Eq. (3.14) in $\mathcal{O}(M_{\text{EIM}}^2)$ operations.

3.4. Inf-Sup Lower Bound: A Modified Successive Constraint Method (SCM).

3.4.1. Lower Bound Formulation. Our objective is to compute a lower bound for the space-time inf-sup constant

$$\beta_N(\mu) \equiv \inf_{w\in\mathcal{X}_\delta} \sup_{v\in\mathcal{Y}_\delta} \frac{\partial \mathcal{G}_\delta(w, u_N(\mu), v; \mu)}{\|w\|_{\mathcal{X}_\delta}\|v\|_{\mathcal{Y}_\delta}}. \tag{3.15}$$

The procedure presented here largely follows the natural-norm successive constraint method (SCM) [14] for linear stationary equations with a few modifications. First, we apply the method to the linearized form of a nonlinear equation; this introduces reduced basis coefficients in the expansion of the linearized form, which in turn requires a particular relationship between SCM control points and reduced basis snapshot points for an efficient computation. Second, we tighten the bounding boxes associated with the SCM method; as we will see shortly, the modification, unlike in the linear case, only moderately increases the cost in the nonlinear case (assuming the reduced basis dimension N is larger than the number of affine expansion coefficients Q^a). Third, we compute all coefficients in space-time spaces; we propose an effective time-marching based computational procedures for the coefficients in the following subsection.

By way of preliminaries, we state two important assumptions of our modified SCM procedure:

- SCM Assumption 1: the SCM anchor point ($\bar{\mu}$) is included in the reduced basis snapshot points.
- SCM Assumption 2: the SCM control points (M^{SCM}) are included in the reduced basis snapshot points.

The roles that the anchor point and control points play in the procedure will become clear shortly. These two assumptions greatly simply the extension of the natural-norm SCM algorithm to nonlinear equations. Both assumptions are verified by construction for the sampling algorithm proposed in Section 4.

We now present the modified SCM procedure. As in the standard SCM, we first fix the supremizing operator to be that computed at an SCM anchor point $\bar{\mu}$, i.e. $S^{\bar{\mu}} : \mathcal{X}_\delta \to \mathcal{Y}_\delta$ such that

$$(S^{\bar{\mu}} w, v)_{\mathcal{Y}_\delta} = \partial \mathcal{G}_\delta(w, u_N(\bar{\mu}), v; \bar{\mu}), \quad \forall w \in \mathcal{X}_\delta,\, v \in \mathcal{Y}_\delta \ .$$

Note that, by SCM Assumption 1, the SCM anchor point is always included in the reduced basis snapshots; thus, $u_N(\bar{\mu}) = u_\delta(\bar{\mu})$ and the supremizing operator $S^{\bar{\mu}}$ is independent of N. Then we construct a lower bound of the inf-sup constant following

$$\begin{aligned}
\beta_N(\mu) &\geq \inf_{w_\delta\in\mathcal{X}_\delta} \frac{\partial \mathcal{G}_\delta(w, u_N(\mu), S^{\bar{\mu}} w; \mu)}{\|w\|_{\mathcal{X}_\delta}\|S^{\bar{\mu}} w\|_{\mathcal{Y}_\delta}} \\
&\geq \left[\inf_{w\in\mathcal{X}_\delta} \frac{\|S^{\bar{\mu}} w\|_{\mathcal{Y}_\delta}}{\|w\|_{\mathcal{X}_\delta}}\right] \left[\inf_{w\in\mathcal{X}_\delta} \frac{\partial \mathcal{G}_\delta(w, u_N(\mu), S^{\bar{\mu}} w; \mu)}{\|S^{\bar{\mu}} w\|^2_{\mathcal{Y}_\delta}}\right] \equiv \beta_N(\bar{\mu})\bar{\beta}^{\bar{\mu}}_N(\mu),
\end{aligned}$$

where we have identified the term in the first bracket as $\beta_N(\bar{\mu})$ and defined the term in the second bracket as $\bar{\beta}^{\bar{\mu}}_N$. Note that $\bar{\beta}^{\bar{\mu}}_N$ is dependent on N as our Fréchet derivative bilinear form changes with our reduced basis approximation $u_N(\mu)$. The goal of natural-norm SCM is to construct lower and upper bounds for the second term in a

manner that permits offline-online computational decomposition. We make modifications to the SCM to improve the tightness of the lower bound.

To facilitate construction of bounds, we first express $\bar{\beta}_N^{\bar{\mu}}$ as

$$\begin{aligned}\bar{\beta}_N^{\bar{\mu}}(\mu) &\equiv \inf_{w\in\mathcal{X}_\delta} \frac{\partial\mathcal{G}_\delta(w,u_N(\mu),S^{\bar{\mu}}w;\mu)}{\|S^{\bar{\mu}}w\|^2_{\mathcal{Y}_\delta}} \\ &= \inf_{w\in\mathcal{X}_\delta}\left[\frac{\mathcal{M}(w,S^{\bar{\mu}}w)+\mathcal{A}_0(w,S^{\bar{\mu}}w)}{\|S^{\bar{\mu}}w\|^2_{\mathcal{Y}_\delta}} + \sum_{q=1}^{Q^a}\Theta_q^a(\mu)\frac{\mathcal{A}_q(w,S^{\bar{\mu}}w)}{\|S^{\bar{\mu}}w\|^2_{\mathcal{Y}_\delta}}\right. \\ &\qquad \left. + \sum_{q=1}^{Q^c}\sum_{k=1}^{N}\Theta_q^c(\mu)\alpha_{Nk}(\mu)\frac{2\mathcal{C}_q(w,\xi_k,S^{\bar{\mu}}w)}{\|S^{\bar{\mu}}w\|^2_{\mathcal{Y}_\delta}}\right].\end{aligned} \tag{3.16}$$

Now we regroup the terms to express the correction factor as a deviation from the linearization at the anchor point $\bar{\mu}$

$$\begin{aligned}\bar{\beta}_N^{\bar{\mu}}(\mu) &= \inf_{w\in\mathcal{X}_\delta}\left[\frac{\partial\mathcal{G}_\delta(w,u(\bar{\mu}),S^{\bar{\mu}}w;\bar{\mu})}{\|S^{\bar{\mu}}w\|^2_{\mathcal{Y}_\delta}} + \sum_{q=1}^{Q^a}(\Theta_q^a(\mu)-\Theta_q^a(\bar{\mu}))\frac{\mathcal{A}_q(w,S^{\bar{\mu}}w)}{\|S^{\bar{\mu}}w\|^2_{\mathcal{Y}_\delta}}\right. \\ &\qquad \left. + \sum_{q=1}^{Q^c}\sum_{k=1}^{N}(\Theta_q^c(\mu)\alpha_{Nk}(\mu)-\Theta_q^c(\bar{\mu})\alpha_{Nk}(\bar{\mu}))\frac{2\mathcal{C}_q(w,\xi_k,S^{\bar{\mu}}w)}{\|S^{\bar{\mu}}w\|^2_{\mathcal{Y}_\delta}}\right] \\ &= 1 + \inf_{w\in\mathcal{X}_\delta}\left[\sum_{q=1}^{Q^a}(\Theta_q^a(\mu)-\Theta_q^a(\bar{\mu}))\frac{\mathcal{A}_q(w,S^{\bar{\mu}}w)}{\|S^{\bar{\mu}}w\|^2_{\mathcal{Y}_\delta}}\right. \\ &\qquad \left. + \sum_{q=1}^{Q^c}\sum_{k=1}^{N}(\Theta_q^c(\mu)\alpha_{Nk}(\mu)-\Theta_q^c(\bar{\mu})\alpha_{Nk}(\bar{\mu}))\frac{2\mathcal{C}_q(w,\xi_k,S^{\bar{\mu}}w)}{\|S^{\bar{\mu}}w\|^2_{\mathcal{Y}_\delta}}\right];\end{aligned}$$

note that the reduced basis coefficients α_{Nk}, $k=1,\ldots,N$, enter the expansion as the coefficients of the trilinear form. The correction factor may then be expressed as

$$\bar{\beta}_N^{\bar{\mu}}(\mu) = 1 + \inf_{z\in Z_N}\mathcal{J}_N(z;\mu),$$

where

$$\mathcal{J}_N(z;\mu) \equiv \sum_{q=1}^{Q^c}\sum_{k=1}^{N}(\Theta_q^c(\mu)\alpha_{Nk}(\mu)-\Theta_q^c(\bar{\mu})\alpha_{Nk}(\bar{\mu}))z_k + \sum_{q=1}^{Q^a}(\Theta_q^a(\mu)-\Theta_q^a(\bar{\mu}))z_{N+q} \tag{3.17}$$

and

$$\begin{aligned}Z_N = \left\{ z\in\mathbb{R}^{Q^cN+Q^a} : \exists w_z\in\mathcal{X}_\delta, z_{(q-1)N+k} = \frac{2\mathcal{C}_q(w_z,\xi_k,S^{\bar{\mu}}w_z)}{\|S^{\bar{\mu}}w_z\|^2_{\mathcal{Y}_\delta}}, k=1,\ldots,N,\right. \\ \left. q=1,\ldots,Q^c\ ;\ z_{Q^cN+q} = \frac{\mathcal{A}_q(w_z,S^{\bar{\mu}}w_z)}{\|S^{\bar{\mu}}w_z\|^2_{\mathcal{Y}_\delta}}, q=1,\ldots,Q^a\right\}.\end{aligned}$$

To compute a lower bound of $\bar{\beta}_N^{\bar{\mu}}(\mu)$, $\bar{\beta}_N^{\bar{\mu},\mathrm{LB}}(\mu)$, we construct $Z_N^{\mathrm{LB}} \supseteq Z_N$. Towards

this end, we first define a ($\bar{\mu}$-dependent) bounding box $B_N^{\bar{\mu}} \subset \mathbb{R}^{Q^c N + Q^a}$ defined by

$$B_{N,(q-1)N+k}^{\bar{\mu}} = \left[\inf_{w \in \mathcal{X}_\delta} \frac{2\mathcal{C}_q(w, \xi_k, S^{\bar{\mu}} w)}{\|S^{\bar{\mu}} w\|_{\mathcal{Y}_\delta}^2}, \sup_{w \in \mathcal{X}_\delta} \frac{2\mathcal{C}_q(w, \xi_k, S^{\bar{\mu}} w)}{\|S^{\bar{\mu}} w\|_{\mathcal{Y}_\delta}^2} \right], \tag{3.18}$$

$$k = 1, \ldots, N, \ q = 1, \ldots, Q^c, \tag{3.19}$$

$$B_{N,Q^c N+q}^{\bar{\mu}} = \left[\inf_{w \in \mathcal{X}_\delta} \frac{\mathcal{A}_q(w, S^{\bar{\mu}} w)}{\|S^{\bar{\mu}} w\|_{\mathcal{Y}_\delta}^2}, \sup_{w \in \mathcal{X}_\delta} \frac{\mathcal{A}_q(w, S^{\bar{\mu}} w)}{\|S^{\bar{\mu}} w\|_{\mathcal{Y}_\delta}^2} \right], \quad q = 1, \ldots, Q^a. \tag{3.20}$$

Clearly, $Z_N \subseteq B_N^{\bar{\mu}}$. We define our Z_N^{LB} as

$$Z_N^{\mathrm{LB}} = \Bigg\{ z \in B_N^{\bar{\mu}} : \sum_{q=1}^{Q^c} \sum_{k=1}^{N} (\Theta_q^c(\mu') \alpha_{Nk}(\mu') - \Theta_q^c(\bar{\mu}) \alpha_{Nk}(\bar{\mu})) z_k \tag{3.21}$$

$$+ \sum_{q=1}^{Q^a} (\Theta_q^a(\mu') - \Theta_q^a(\bar{\mu})) z_{N+q} \geq \inf_{z \in Z_N} \mathcal{J}_N(z; \mu'), \forall \mu' \in M^{\mathrm{SCM}} \Bigg\}, \tag{3.22}$$

where $M^{\mathrm{SCM}} \subset \mathcal{D}$ is a set of SCM control points. By SCM Assumption 2, our SCM control point, $\mu' \in M^{\mathrm{SCM}}$, is a reduced basis snapshot. This implies that, once the constraint $\inf_{z \in Z_N} \mathcal{J}_N(z; \mu') = \beta_N^{\bar{\mu}}(\mu') - 1$ is computed at the k'-th reduced basis sampling point μ', it need not be updated as N increases because $\alpha_{Nk}(\mu_{k'}) = 0$, $k = k' + 1, \ldots, N$, due to the hierarchical construction of the basis. To evaluate a lower bound for the inf-sup correction factor, we solve a linear program:

$$\bar{\beta}_N^{\bar{\mu},\mathrm{LB}}(\mu) = 1 + \inf_{z \in Z_N^{\mathrm{LB}}} \mathcal{J}_N(z; \mu), \tag{3.23}$$

where $\mathcal{J}_N$ is the function defined in Eq. (3.17). As regards the sharpness of the modified SCM inf-sup lower bound, we have the following proposition:

PROPOSITION 3.7. *Given the same set of SCM control points, the lower bound for the inf-sup correction factor presented above, $\bar{\beta}_N^{\bar{\mu},\mathrm{LB}}(\mu)$, is sharper than the original bound [14], here denoted by $\bar{\beta}_N^{\bar{\mu},\mathrm{LB,orig}}(\mu)$, i.e.*

$$\bar{\beta}_N^{\bar{\mu}}(\mu) \geq \bar{\beta}_N^{\bar{\mu},\mathrm{LB}}(\mu) \geq \bar{\beta}_N^{\bar{\mu},\mathrm{LB,orig}}(\mu). \tag{3.24}$$

Proof. The only difference in the original formulation [14] and the above formulation is the choice of the bounding box. Thus, to prove Eq. (3.24), it suffices to show that

$$B_{N,k}^{\bar{\mu}} \subset B_{N,k}^{\bar{\mu},\mathrm{orig}}, \quad k = 1, \ldots, Q^c N + Q^a.$$

The original SCM bounding box is given by[5]

$$B_{N,k}^{\bar{\mu},\mathrm{orig}} = \left[-\frac{\gamma_k}{\beta(\bar{\mu})}, \frac{\gamma_k}{\beta(\bar{\mu})} \right],$$

where

$$\gamma_k = \sup_{w \in \mathcal{X}_\delta} \frac{\|T_k w\|_{\mathcal{Y}_\delta}}{\|w\|_{\mathcal{X}_\delta}}, \tag{3.25}$$

[5]Originally presented for Galerkin formulation; here generalized for Petrov-Galerkin formulation.

and $T_k : \mathcal{X}_\delta \to \mathcal{Y}_\delta$, $k = 1, \ldots, Q^c N + Q^a$, satisfy

$$(T_{(q-1)N+k} w, v)_{\mathcal{Y}_\delta} = 2\mathcal{C}_q(w, \xi_k, v), \quad \forall w \in \mathcal{X}_\delta,\ v \in \mathcal{Y}_\delta,\ k = 1, \ldots, N,\ q = 1, \ldots, Q^c,$$
$$(T_{Q^c N + k} w, v)_{\mathcal{Y}_\delta} = \mathcal{A}_k(w, v), \quad \forall w \in \mathcal{X}_\delta,\ v \in \mathcal{Y}_\delta,\ k = 1, \ldots, Q^a.$$

Let us first show that the upper limit of $B^{\bar\mu}_{N,k}$ is less than that of $B^{\bar\mu,\mathrm{orig}}_{N,k}$ for $k = Q^c N + 1, \ldots, Q^c N + Q^a$:

$$\begin{aligned}\sup_{w\in\mathcal{X}_\delta} \frac{\mathcal{A}_{k-Q^cN}(w, S^{\bar\mu} w)}{\|S^{\bar\mu} w\|^2_{\mathcal{Y}_\delta}} &\le \sup_{w\in\mathcal{X}_\delta} \frac{|(T_k w, S^{\bar\mu} w)_{\mathcal{Y}_\delta}|}{\|S^{\bar\mu} w\|^2_{\mathcal{Y}_\delta}} \le \sup_{w\in\mathcal{X}_\delta} \frac{\|T_k w\|_{\mathcal{Y}_\delta}}{\|S^{\bar\mu} w\|_{\mathcal{Y}_\delta}} \\ &\le \sup_{w\in\mathcal{X}_\delta} \frac{\|T_k w\|_{\mathcal{Y}_\delta}}{\|w\|_{\mathcal{X}_\delta}} \left(\inf_{w\in\mathcal{X}_\delta} \frac{\|S^{\bar\mu} w\|_{\mathcal{Y}_\delta}}{\|w\|_{\mathcal{X}_\delta}} \right)^{-1} = \frac{\gamma_k}{\beta(\bar\mu)};\end{aligned}$$

we recognize that the final expression is precisely the upper limit of $B^{\bar\mu,\mathrm{orig}}_{N,k}$. Moreover, the lower limit of $B^{\bar\mu}_{N,k}$ is greater than that of $B^{\bar\mu,\mathrm{orig}}_{N,k}$ because

$$\inf_{w\in\mathcal{X}_\delta} \frac{\mathcal{A}_q(w, S^{\bar\mu} w)}{\|S^{\bar\mu} w\|^2_{\mathcal{Y}_\delta}} \ge - \sup_{w\in\mathcal{X}_\delta} \frac{|(T_k w, S^{\bar\mu} w)_{\mathcal{Y}_\delta}|}{\|S^{\bar\mu} w\|^2_{\mathcal{Y}_\delta}} \ge -\frac{\gamma_k}{\beta(\bar\mu)}.$$

(The same arguments for the upper and lower bounds follow for $k = 1, \ldots, Q^c N$.) Thus, we have $B^{\bar\mu}_{N,k} \subset B^{\bar\mu,\mathrm{orig}}_{N,k}$, $k = 1, \ldots, Q^c N + Q^a$, which is the desired result. □

We remark that the modified SCM improve the sharpness without a significant increase in the computational cost for nonlinear equations:

Remark 3.8. For linear equations (in which the linearized form is independent of the reduced basis approximation), the original bounding box construction procedure [14] is computationally less expensive than the new procedure as the factors γ_k defined in Eq. (3.25) are independent of the anchor point $\bar\mu$; i.e. the γ_k, $k = Q^c N + 1, \ldots, Q^c N + Q_a$ (with $N = 0$), need to be computed only once for all hp-partitions. However, for equations with quadratic nonlinearity, γ_k, $k = 1, \ldots, Q^c N$, arising from the linearization of the quadratic term would have to be computed for each partition separately. Thus, the computational cost of the new procedure is comparable to that of the original formulation, while providing a tighter inf-sup lower bound.

3.4.2. Offline-Online Procedure. We first compute an upper bound of the inf-sup correction factor to facilitate the SCM sampling process. The construction is identical to the original procedure [14]; here we present a brief description for completeness. An upper bound for the correction factor is constructed by choosing $Z^{\mathrm{UB}}_N \subseteq Z_N$. We simply choose

$$\begin{aligned}Z^{\mathrm{UB}}_N = \Bigg\{ z \in \mathbb{R}^{Q^cN+Q^a} : z_{(q-1)N+k} &= \frac{\mathcal{C}_q(w', \xi_k, S^{\bar\mu} w')}{\|S^{\bar\mu} w'\|^2_{\mathcal{Y}_\delta}},\ k = 1, \ldots, N,\ q = 1, \ldots, Q^c; \\ z_{Q^cN+j} &= \frac{\mathcal{A}_j(w', S^{\bar\mu} w')}{\|S^{\bar\mu} w'\|^2_{\mathcal{Y}_\delta}},\ j = 1, \ldots, Q^a; \\ w' &= \arg \inf_{w\in\mathcal{X}} \frac{\partial \mathcal{G}_\delta(w, u^N(\mu'), S^{\bar\mu} w; \mu')}{\|S^{\bar\mu} w\|^2_{\mathcal{Y}_\delta}}, \mu' \in M^{\mathrm{SCM}} \Bigg\}.\end{aligned}$$

In other words, $z \in Z_N^{\rm UB}$ consists of the forms evaluated about the infimizer at a given SCM control point. Note that every element in this set must be updated when N is increased, i.e. compute the new term arising from the addition of the trilinear form evaluated about the new linearization point. Our upper bound for the inf-sup correction factor is the solution of a linear program

$$\bar{\beta}_N^{\bar{\mu},\rm UB}(\mu) = 1 + \inf_{z \in Z_N^{\rm LB}} \mathcal{J}_N(z;\mu), \tag{3.26}$$

where again $\mathcal{J}_N$ is the function defined in Eq. (3.17).

The *online-offline* computational decomposition is apparent from the construction. In the *offline* stage, we compute

- the inf-sup constant at the anchor point $\bar{\mu}$, $\beta_N(\bar{\mu})$;
- the SCM bounding box $B_N^{\bar{\mu}} \subset \mathbb{R}^{Q^c N + Q^a}$ defined by Eqs. (3.20) and (3.19);
- and the SCM correction factors $\bar{\beta}_N^{\bar{\mu}}(\mu')$, $\mu' \in M^{\rm SCM}$, defined in Eq. (3.16) (for $Z_N^{\rm LB}$) and its infimizers (for $Z_N^{\rm UB}$) evaluated at the SCM control points.

In the *online* stage, we simply solve the linear programs Eqs. (3.23) and (3.26) to obtain a lower bound $\bar{\beta}_N^{\bar{\mu},\rm LB}(\mu)$ and an upper bound $\bar{\beta}_N^{\bar{\mu},\rm UB}(\mu)$, respectively, for a select μ. The inf-sup lower and upper bounds are given by $\beta_N^{\rm LB}(\mu) = \beta_N(\bar{\mu})\bar{\beta}_N^{\bar{\mu},\rm LB}(\mu)$ and $\beta_N^{\rm UB}(\mu) = \beta_N(\bar{\mu})\bar{\beta}_N^{\bar{\mu},\rm UB}(\mu)$.

Before concluding this discussion on the construction of the inf-sup lower bound, let us clarify computations involved in the offline construction of $Z_N^{\rm LB}$. First, evaluation of the inf-sup constant at the SCM anchor point $\bar{\mu}$, $\beta_N(\bar{\mu})$, requires the minimum eigenvalue of a generalized symmetric eigenproblem $\mathbf{P}\boldsymbol{w} = \lambda \mathbf{Q}\boldsymbol{w}$ with

$$\mathbf{P} = \mathbf{G}(\bar{\mu})^T \mathbf{Y}^{-1} \mathbf{G}(\bar{\mu}) \tag{3.27}$$

$$\mathbf{Q} = \mathbf{X} \tag{3.28}$$

and setting $\beta_N(\bar{\mu}) = \sqrt{\lambda_{\min}}$. Here, the matrices, all of dimension $\mathbb{R}^{\mathcal{N}\times\mathcal{N}}$, are given by $\mathbf{G}(\bar{\mu})_{ij} = \partial\mathcal{G}(\phi_j, u(\bar{\mu}), \phi_i; \bar{\mu})$, $\mathbf{Y}_{ij} = (\phi_j, \phi_i)_{\mathcal{Y}_\delta}$, and $\mathbf{X}_{ij} = (\phi_j, \phi_i)_{\mathcal{X}_\delta}$. The set $\{\phi_i\}_{i=1}^{\mathcal{N}}$ is a space-time finite element basis. Effectively locating the minimum eigenvalue by a Krylov method requires generation of a Krylov space $\mathcal{K}(\mathbf{P}^{-1}\mathbf{Q})$. Application of $\mathbf{P}^{-1} = \mathbf{G}(\bar{\mu})^{-1}\mathbf{Y}\mathbf{G}(\bar{\mu})^{-T}$ requires solution to the adjoint problem ($\mathbf{G}(\bar{\mu})^{-T}$), multiplication by $\mathbf{Y}$, followed by the solution to the linearized forward problem ($\mathbf{G}(\bar{\mu})^{-1}$); all of these operations can be performed in a time-marching manner, not requiring fully-coupled space-time solves.

The construction of the bounding boxes $B_{N,k}^{\bar{\mu}}$, $k = 1, \ldots, Q^c N$, defined by Eq. (3.19) require the extreme eigenvalues of $Q^c N$ eigenproblems $\mathbf{P}\boldsymbol{w} = \lambda\mathbf{Q}\boldsymbol{w}$ with

$$\begin{aligned} \mathbf{P} &= \mathbf{G}(\bar{\mu})^T \mathbf{Y}^{-1} \mathbf{C}_q(\xi_k) + \mathbf{C}_q(\xi_k)^T \mathbf{Y}^{-1} \mathbf{G}(\bar{\mu}) \\ \mathbf{Q} &= \mathbf{G}(\bar{\mu})^T \mathbf{Y}^{-1} \mathbf{G}(\bar{\mu}), \end{aligned} \tag{3.29}$$

where $\mathbf{C}_q(\xi_k) = \mathcal{C}_q(\phi_j, \xi_k, \phi_i)$ and $\{\xi_k\}_{k=1}^N$ is the $\mathcal{X}_\delta$-orthonormalized reduced basis set. The maximum and minimum eigenvalues correspond to the upper and lower limits, respectively, of the bounding box. Similarly, the bounding boxes $B_{N,Q^cN+k}^{\bar{\mu}}$, $k = 1, \ldots, Q^a$ defined by Eq. (3.20) require extreme eigenvalues of Q^a eigenproblems $\mathbf{P}\boldsymbol{w} = \lambda\mathbf{Q}\boldsymbol{w}$ with

$$\begin{aligned} \mathbf{P} &= \frac{1}{2}\left[\mathbf{G}(\bar{\mu})^T \mathbf{Y}^{-1} \mathbf{A}_k + \mathbf{A}_k^T \mathbf{Y}^{-1} \mathbf{G}(\bar{\mu})\right] \\ \mathbf{Q} &= \mathbf{G}(\bar{\mu})^T \mathbf{Y}^{-1} \mathbf{G}(\bar{\mu}), \end{aligned} \tag{3.30}$$

where $(\mathcal{A}_k)_{ij} = \mathcal{A}_k(\phi_j, \phi_i)$. The extreme eigenvalues for the bounding boxes can be effectively approximated in a Krylov space $\mathcal{K}(\mathbf{Q}^{-1}\mathbf{P})$ (assuming the minimum eigenvalue is negative and is far from the origin). The application of $\mathbf{Q}^{-1}$ is identical to the application of $\mathbf{P}^{-1}$ for the inf-sup calculation; the operation permits time-marching.

The evaluation of the correction factor at a SCM control point $\mu' \in M^{\rm SCM}$, $\bar{\beta}_N^{\bar{\mu}}(\mu')$, by Eq. (3.16) requires the minimum eigenvalue of $\mathbf{P}\boldsymbol{w} = \lambda\mathbf{Q}\boldsymbol{w}$ with

$$\mathbf{P} = \frac{1}{2}\left[\mathbf{G}(\bar{\mu})^T\mathbf{Y}^{-1}\mathbf{G}(\mu') + \mathbf{G}(\mu')\mathbf{Y}^{-1}\mathbf{G}(\bar{\mu})\right]$$
$$\mathbf{Q} = \mathbf{G}(\bar{\mu})^T\mathbf{Y}^{-1}\mathbf{G}(\bar{\mu}).$$

Effectively locating the minimum eigenvalue requires a Krylov space $\mathcal{K}(\mathbf{Q}\mathbf{P}^{-1})$. Unfortunately, the application of $\mathbf{P}^{-1}$ cannot be performed in a time-marching manner in general. However, the eigenvalue of interest is one of the extreme eigenvalues, thus we have found that we can seek the eigenvalue in a Krylov space $\mathcal{K}(\mathbf{Q}^{-1}\mathbf{P})$, which allows for time-marching computation, and obtain a reasonable (albeit slower) convergence.

3.5. L^4-$\mathcal{X}_\delta$ Sobolev Embedding Constant. The final piece required for the evaluation of the BRR error bound is the L^4-$\mathcal{X}_\delta$ space-time Sobolev embedding constant, Eq. (3.10). To our knowledge, the embedding constant cannot be evaluated analytically due to the nonlinearity of the L^4 norm. However, a few numerical techniques for estimating the constant have been devised. Here, we employ the fixed point algorithm of Deparis [8] in the space-time context. We have found the algorithm converges more rapidly and reliably than the Newton-homotopy algorithm of Veroy and Patera [26]. For the purpose of relating numerical results with analysis, we restrict ourselves to a Cartesian-product domain, $\Omega = \prod_{i=1}^d [0, L_i] \subset \mathbb{R}^d$ and take $V = H_0^1(\Omega)$. However, the technique used here applies to arbitrary domains, and we expect properties of the L^4-$\mathcal{X}_\delta$ space-time embedding constant observed for the particular case to be retained in more general cases.

First, we analyze a closely related linear problem: L^2-$\mathcal{X}$ embedding. A bound for the embedding constant can be found analytically using Fourier decomposition in space and time. (The technique is identical to that used in our previous work [28]; however, the temporal Fourier modes here are different as functions in $\mathcal{X}$ do not vanish at $t = 0$.) The L^2-$\mathcal{X}$ constant is bounded by

$$\rho_{L^2\text{-}\mathcal{X}} \equiv \sup_{w\in\mathcal{X}} \frac{\|w\|_{L^2(I;L^2(\Omega))}}{\|w\|_{\mathcal{X}}} \le \left(\sup_{w\in\mathcal{X}} \frac{\|w\|^2_{L^2(I;L^2(\Omega))}}{\|\dot{w}\|^2_{L^2(I;V')} + \|w\|^2_{L^2(I;V)}}\right)^{1/2}$$
$$\le \frac{1}{\pi\sqrt{\prod_{i=1}^d L_i^{-2}}}.$$

Note that the L^2-$\mathcal{X}$ embedding constant is bounded independent of the final time T.

We now (computationally) demonstrate that the L^2-$\mathcal{X}_\delta$ embedding constant for our DG $\mathcal{X}_\delta$ norm is largely independent of the final time T as well as the discretization resolution — both in space and time. To compute the embedding constant, we seek the maximum eigenvalue of a space-time eigenproblem: find $(w, \lambda) \in \mathcal{X}_\delta \times \mathbb{R}$ such that $\|w\|_{\mathcal{X}_\delta} = 1$ and

$$(w, v)_{L^2(I;L^2(\Omega))} = \lambda(w, v)_{\mathcal{X}_\delta}, \quad \forall v \in \mathcal{X}_\delta \ ; \tag{3.31}$$

(a) L^2-$\mathcal{X}_\delta$ mesh dependence ($T = 1$)

K	$\lvert\mathcal{T}_h\rvert = 32$	128	512	2048
4	0.3170	0.3089	0.3064	0.3060
8	0.3170	0.3089	0.3064	0.3060
16	0.3170	0.3089	0.3064	0.3060

(b) L^2-$\mathcal{X}_\delta$ T-dependence

T	$\rho_{L^2\text{-}\mathcal{X}_\delta}$
0.5	0.3023
1.0	0.3089
2.0	0.3110

(c) L^4-$\mathcal{X}_\delta$ mesh dependence ($T = 1$)

K	$\lvert\mathcal{T}_h\rvert = 32$	128	512	2048
4	0.4820	0.4916	0.4947	0.4950
8	0.4850	0.4946	0.5002	0.5009
16	0.4829	0.4929	0.5009	0.5026

(d) L^4-$\mathcal{X}_\delta$ T-dependence

T	ρ
0.5	0.4929
1.0	0.4946
2.0	0.4916

TABLE 3.1

Variation in the L^2-$\mathcal{X}_\delta$ and L^4-$\mathcal{X}_\delta$ space-time Sobolev embedding constant with the space-time discretization and the final time T. The computation is carried out on the space-time domain $\Omega \times I \equiv ((0,4)\times(0,1))\times(0,T]$ discretized by $\lvert\mathcal{T}_h\rvert$ $\mathbb{P}^2$ conforming finite elements in space and K $\mathbb{P}^2$ DG elements in time. The results on Tables (b) and (d) are obtained on the $\lvert\mathcal{T}_h\rvert = 32$ spatial mesh.

we then evaluate the L^2-$\mathcal{X}_\delta$ embedding constant, $\rho_{L^2\text{-}\mathcal{X}_\delta} = \sqrt{\lambda_{\max}}$. Table 3.1(a) shows the variation in the embedding constant for a several combinations of spatial and temporal discretizations for the final time of $T = 1.0$. The result suggests that the embedding constant is only weakly dependent on both the spatial and temporal discretizations. Table 3.1(b) shows that the embedding constant is also only weakly dependent on the final time T; the constant exhibits less than 3% variation as T varies from 0.5 to 2.0. In particular, the L^2-$\mathcal{X}_\delta$ embedding constant appears to be bounded by approximately 0.3, which is in a good agreement with the (continuous) L^2-$\mathcal{X}$ embedding bound of approximately 0.2996 for this space-time domain, $\Omega \times I \equiv ((0,4)\times(0,1))\times(0,1]$.[6] In contrast, the Sobolev embedding constant for a space-time norm associated with the Crank-Nicolson scheme is (provably) weakly dependent on the final time T, and the supremizer of the embedding constant is also dependent on the number of time steps K [28].

We finally (computationally) demonstrate that the L^4-$\mathcal{X}_\delta$ embedding constant is only weakly dependent of the final time T and the discretization resolution. We employ the fixed-point algorithm of Deparis [8] to estimate the embedding constant; here we briefly outline the algorithm. We first define an operator $z : \mathcal{X}_\delta \to L^4(I; L^4(\Omega))$ given by $z(w) = \|w\|^{-2}_{L^4(I;L^4(\Omega))} w^2$. We then introduce an eigenproblem: for a given $\xi \in \mathcal{X}_\delta$, find $(w, \lambda) \in \mathcal{X}_\delta \times \mathbb{R}$ such that $\|w\|_{\mathcal{X}_\delta} = 1$ and

$$\int_I \int_\Omega z(\xi) w_i v_i dx dt = \lambda_{\max}(w, v)_{\mathcal{X}_\delta}, \quad \forall v \in \mathcal{X}_\delta; \tag{3.32}$$

we denote the maximum eigenvalue and the associated eigenfunction, parametrized by $z(\xi)$, by $\lambda_{\max}(z(\xi))$ and $w_{\max}(z(\xi))$, respectively. The L^4-$\mathcal{X}_\delta$ supremizer, ξ^*, is the fixed point $\xi^* = w_{\max}(z(\xi^*))$ and the embedding constant is $\rho = \sqrt{\lambda_{\max}(z(\xi^*))}$. We thus have a fixed-point algorithm [8]: initialize $\xi^0 = 1$ and set $k = 0$; for $k \geq 1$, set $\xi^k = w_{\max}(z(\xi^{k-1}))$ and $\lambda^k = \lambda_{\max}(z(\xi^{k-1}))$. The computational results in Tables 3.1(c) and 3.1(d) show that the L^4-$\mathcal{X}_\delta$ embedding constant is only weakly dependent on the discretization resolution and the final time, exhibiting less than 5%

[6] Note that that the embedding constants $\rho_{L^2\text{-}\mathcal{X}}$ and $\rho_{L^2\text{-}\mathcal{X}_\delta}$ are associated with two different norms, and hence in general the upper bound of $\rho_{L^2\text{-}\mathcal{X}}$ does not serve as an upper bound of $\rho_{L^2\text{-}\mathcal{X}_\delta}$.

variation. The behavior implies that the embedding constant need to be evaluated for a single final time. (We use $\rho = 0.51$ for all our later numerical results.)

We make a few comments as regard the computation of the embedding constant. The computation of the L^4-$\mathcal{X}_\delta$ embedding constant by the fixed-point algorithm of Deparis [8] requires solution to multiple eigenproblem of the form Eq. (3.32). An effective solution of the eigenproblem via a Krylov method requires the action of the inverse of the $\mathcal{X}_\delta$ operator. (This requirement also applies to the L^2-$\mathcal{X}_\delta$ eigenproblem, Eq. (3.31).) Although the matrix $\mathbf{X} \in \mathbb{R}^{\mathcal{N}\times\mathcal{N}}$ with $\mathbf{X}_{ij} = (\phi_j, \phi_i)_{\mathcal{X}_\delta}$ (where $\{\phi_i\}_{i=1}^{\mathcal{N}}$ is a space-time finite element basis) is a block tridiagonal matrix, we can form a block bidiagonal decomposition of the matrix by using the fact that $\mathcal{X}_\delta$ is the natural norm associated with the heat equation (see Remark 2.2). Namely, we have

$$\mathbf{X} = \mathbf{G}_{\text{heat}}^T \mathbf{Y}^{-1} \mathbf{G}_{\text{heat}} \quad \text{and} \quad \mathbf{X}^{-1} = \mathbf{G}_{\text{heat}}^{-1} \mathbf{Y} \mathbf{G}_{\text{heat}}^{-T},$$

where $\mathbf{G}_{\text{heat},ij} = \dot{\mathcal{M}}_\delta(\phi_j, \phi_i) + \mathcal{A}_0(\phi_j, \phi_i) + (\phi_j(t_+^0), \phi_i(t_+^0))$. With the decomposition, the action of $\mathbf{X}^{-1}$ can be computed in a time-marching manner without requiring a fully-coupled space-time solve. Namely, we first perform the backward (adjoint) solve starting from the final time ($\mathbf{G}_{\text{heat}}^{-T}$), apply $\mathbf{Y}$, and then perform the linearized forward solve ($\mathbf{G}_{\text{heat}}^{-1}$).

3.6. Output Approximation and Certification. Let $\ell \in \mathcal{X}_\delta'$ be a output functional of interest. For simplicity we consider a linear output functional in this work; we refer to Deparis [8] for a treatment of quadratic functional outputs within a (space-only, not space-time) BRR framework.

For approximation, we appeal to the linearity of the functional and $u_N(\mu) = \xi_k \alpha_{Nk}(\mu)$ to express the reduced basis output as

$$\ell(u_N(\mu)) = \ell_N(\xi_k)\alpha_{Nk}(\mu).$$

In the *offline* stage, we compute $\ell_N(\xi_k)$, $k = 1, \ldots, N$; in the *online* stage we evaluate the above expression.

For certification, we employ a simple error bound that does not require the solution of the dual problem. Namely, we construct our output error bound according to

$$\begin{aligned} |\ell(u_\delta(\mu);\mu) - \ell(u_N(\mu);\mu)| = |\ell(e;\mu)| &\le \|\ell(\,\cdot\,;\mu)\|_{\mathcal{X}_\delta'} \|e(\mu)\|_{\mathcal{X}_\delta} \\ &\le \|\ell(\,\cdot\,;\mu)\|_{\mathcal{X}_\delta'} \Delta_N(\mu) \equiv \Delta_N^\ell(\mu), \end{aligned}$$

where we recall $\|\ell(\,\cdot\,;\mu)\|_{\mathcal{X}_\delta'} \equiv \sup_{w\in\mathcal{X}_\delta} \ell(w;\mu)/\|w\|_{\mathcal{X}_\delta}$ and $\|\Delta_N(\mu)\|$ is the $\mathcal{X}_\delta$-norm BRR error bound defined in Eq. (3.9).

Remark 3.9. A primal-dual formulation would yield a sharper error bound; for its application within the BRR formulation, see, e.g., Veroy and Patera [26] and Deparis [8].

4. *hp*-Adaptive Sampling Algorithm. We now describe an *hp* parameter-domain decomposition and parameter sampling strategy employed in the offline stage. The algorithm is motivated by the following observations. First, we note that the (modified) natural norm SCM algorithm, which uses a fixed supremizing operator computed about the anchor point, provides positive inf-sup lower bounds only in the neighborhood of the anchor point; the bound becomes negative (and hence meaningless) if the linearized form evaluated at the anchor point is significantly different —

due to the change either directly in the parameter μ or indirectly in the linearization point $u_N(\mu)$ — and the supremizing operator becomes ineffective. Second, the number of terms in the expansion of the linearized form considered in the SCM formulation depends on the dimension of the reduced basis space N; in order to control the number of space-time eigenvalue problems in the offline stage and the size of the linear program in the online stage, it is advantageous to reduce the size of each reduced basis space. Third, the inability of the supremizing operator at an anchor point to produce a positive inf-sup constant at another parameter point indicates that the dynamics is in fact sufficiently different at the two parameter points; we thus conjecture that two different reduced basis spaces are required to efficiently approximate the two different dynamics. The above observations suggest an application of an *hp* parameter-domain decomposition.

We first present our algorithm for the construction of a certified reduced basis model over a *single* parameter domain in the neighborhood of the parameter sampling point $\bar{\mu}$ that serves as the SCM anchor point. The inputs to the algorithm are

- $\Xi \in [\mathcal{D}]^{N_{\text{train}}}$: a set of N_{train} training points that sufficiently covers $\mathcal{D}$;
- $\bar{\mu}$: parameter "anchor" point;
- $\Delta^{\text{tol}} \in \mathbb{R}^+$: error bound tolerance;
- $\bar{\beta}_N^{\bar{\mu},\text{LB,tol}} \in (0,1)$, $\beta_N^{\text{gap,tol}} \in \mathbb{R}^+$: threshold parameters.

The role of the threshold parameters will become clear shortly. The outputs of the algorithm are

- $\Xi^{\text{certified}}(\bar{\mu}) \subset \Xi$: a training set representation of the certified parameter region such that $\Delta(\mu) \le \Delta^{\text{tol}}$, $\forall \mu \in \Xi^{\text{certified}}(\bar{\mu})$.
- The (inner products of the) Riesz pieces for Petrov-Galerkin reduced basis approximation by Eq. (3.4)
- The quantities required for the EIM-based residual dual norm evaluation by Eq. (3.14)
- The SCM pieces: inf-sup constant at the anchor point $\beta_N(\bar{\mu})$ defined by Eq. (3.15); the SCM bounding boxes $B^{\bar{\mu}}_{Q^c N+q}$, $q = 1,\ldots,Q^a$, defined by Eq. (3.20) and $B^{\bar{\mu}}_{(q-1)N+k}$, $k = 1,\ldots,N$, $q = 1,\ldots,Q^c$, defined by Eq. (3.19); SCM control points $M^{\text{SCM}} \subset \Xi$; and the inf-sup correction factors evaluated at the SCM control points $\bar{\beta}_N^{\bar{\mu}}(\mu)$, $\mu \in M^{\text{SCM}}$, defined by Eq. (3.16).

The algorithm for constructing a certified reduced basis model over a single *hp*-partition, from hereon denoted as Algorithm 1, is summarized as follows:

1. Set $\mu_1 = \bar{\mu}$, which serves as the SCM "anchor point"; set $N = 1$.
2. Obtain the finite element solution $u_\delta(\bar{\mu})$ by solving Eq. (2.10); normalize the solution and set $\xi_1 = u_\delta(\bar{\mu})/\|u_\delta(\bar{\mu})\|_{\mathcal{X}_\delta}$.
3. Compute the Riesz pieces and their inner products required for the Petrov-Galerkin reduced basis approximation.
4. Compute the quantities required for the EIM-based residual dual norm evaluation.
5. Compute the inf-sup constant at the anchor point, $\beta_N(\bar{\mu})$.
6. Construct SCM bounding intervals for the bilinear forms $\mathcal{A}_q(\cdot,\cdot)$, $B^{\bar{\mu}}_{Q^c+q}$, $q = 1,\ldots,Q^a$, and that for the linearized quadratic form $\mathcal{C}_q(\cdot,\xi_1,\cdot)$, $B^{\bar{\mu}}_q$, $q = 1,\ldots,Q^c$.
7. Obtain RB approximation and BRR certification for each $\mu \in \Xi$; record the BRR normalized residual $\tau_N(\mu)$, the error bound $\Delta_N(\mu)$, the lower bound of the inf-sup correction factor $\bar{\beta}_N^{\bar{\mu},\text{LB}}(\mu)$, and the upper bound of the inf-sup correction factor $\bar{\beta}_N^{\bar{\mu},\text{UB}}(\mu)$ for each $\mu \in \Xi$.

8. If $\max_{\{\mu\in\Xi:\bar{\beta}_N^{\bar{\mu},\mathrm{LB}}(\mu)>\bar{\beta}_N^{\bar{\mu},\mathrm{LB,tol}}\}} \Delta_N(\mu) < \Delta^{\mathrm{tol}}$, we are done with this subdomain; set $\Xi^{\mathrm{certified}}(\bar{\mu}) \equiv \{\mu \in \Xi : \bar{\beta}_N^{\bar{\mu},\mathrm{LB}}(\mu) > \bar{\beta}_N^{\bar{\mu},\mathrm{LB,tol}}\}$ and terminate.
9. Within a set of points having the inf-sup lower bound above the tolerance ($\bar{\beta}_N^{\bar{\mu},\mathrm{LB}} \geq \bar{\beta}_N^{\bar{\mu},\mathrm{LB,tol}}$), choose the point with the maximum BRR normalized residual, i.e. $\mu_{N+1} = \arg\max_{\bar{\beta}_N^{\bar{\mu},\mathrm{LB}}(\mu)>\bar{\beta}_N^{\bar{\mu},\mathrm{LB,tol}}} \tau_N(\mu)$ (or $\Delta^N(\mu)$ if $\max_{\mu\in\Xi}(\tau_N(\mu)) < 1$, $\forall \mu \in \Xi$); increment the size of the reduced basis set, $N \leftarrow N + 1$.
10. Compute the finite element solution $u_\delta(\mu_N)$ and $\mathcal{X}_\delta$-orthonormalize it with respect to $\xi_1, \ldots, \xi_{N-1}$ to generate ξ_N.
11. Update the Riesz pieces required for Petrov-Galerkin projection and the variables required for residual dual norm evaluation.
12. Construct the SCM bounding interval for $\mathcal{C}_q(\cdot, \xi_N, \cdot)$, $B^{\bar{\mu}}_{(q-1)N+N}$, $q = 1, \ldots, Q^c$.
13. If the SCM gap is sufficiently large in the sense that $(\bar{\beta}_{N-1}^{\bar{\mu},\mathrm{UB}}(\mu_N) - \bar{\beta}_{N-1}^{\bar{\mu},\mathrm{LB}}(\mu_N))/\bar{\beta}_{N-1}^{\bar{\mu},\mathrm{LB}}(\mu_N) > \beta_N^{\mathrm{gap,tol}}$, then add μ_N to the set of SCM control points ($M^{\mathrm{SCM}} \leftarrow \{M^{\mathrm{SCM}}, \mu_N\}$) and compute the associated correction factor $\bar{\beta}_N^{\bar{\mu}}(\mu_N)$.
14. Update Z_N^{UB} to account for $\mathcal{C}$ linearized about ξ_N.
15. Go to Step 7.

This algorithm constructs a certified reduced basis model in the neighborhood of the anchor point $\bar{\mu}$. Note that we do not partion the parameter domain *a priori*: we initially apply the algorithm to the (full) training set Ξ associated with the (full) domain $\mathcal{D}$; we then, at the termination of the algorithm, obtain an implicitly defined subdomain based on the positivity (more precisely, threshold) constraint on the inf-sup lower bound. As the linearized form (and hence the inf-sup bound) changes with the number of reduced basis functions, the certified subdomain changes accordingly. The reduced basis snapshots are chosen in a greedy manner based on the subdomain definition at each iteration; due to the change in the subdomain with N, a snapshot computed in the earlier stage could fall outside of the final subdomain.

To construct a set of certified reduced basis models that enable reduced basis approximation and certification over the *entire* parameter domain $\mathcal{D}$, we recursively use Algorithm 1. Namely, the algorithm, referred to as Algorithm 2, is summarized as follows:

1. Set $\bar{\mu}_1 = \mathrm{centroid}(\mathcal{D})$; set $k = 1$.
2. Execute Algorithm 1; Set the new working region $\Xi \leftarrow \Xi \setminus \Xi^{\mathrm{certified}}(\bar{\mu}_k)$.
3. If $\Xi = \emptyset$, terminate.
4. Pick $\bar{\mu}_{k+1} = \arg\min_{\mu\in\Xi} \beta_N^{\mathrm{LB}}(\mu)$ with the lowest $\beta_N^{\mathrm{LB}}(\mu)$ prediction based on the RB/SCM approximation over region k; set $k \leftarrow k + 1$.
5. Go to Step 2.

In words, we first pick the centroid of the domain as the SCM snchor point and construct a reduced basis model which certifies the solution in the neighborhood of the point, $\Xi^{\mathrm{certified}}(\bar{\mu}_1)$; we then choose the next SCM anchor point to be the point with the smallest inf-sup lower bound lower bound and construct another reduced basis model about the point. Note that the size of each domain is implicitly defined by the positivity (more precisely, threshold) constraint on the inf-sup lower bound approximated by the SCM that uses a fixed supremizing operator; however, as noted in the beginning of the section, we conjecture that the *hp*-partioning also facilitates construction of more efficient reduced basis approximation for each parameter region.

In the online stage, given a parameter value μ, we evaluate the reduced basis approximation as follows:

1. Create an ordered set $(j_1, \ldots, j_J)$ such that $\|\mu - \bar{\mu}_{j_1}\|_{\ell^2}, \ldots, \|\mu - \bar{\mu}_{j_J}\|_{\ell^2}$ is a non-decreasing sequence. Set $k = 1$.
2. Use the reduced basis model associated with the subdomain j_k (i.e. the subdomain with the k-th nearest anchor point) to obtain $u_N(\mu)$.
3. Compute the BRR error bound $\Delta_N(\mu)$
   - if $\Delta_N(\mu) \leq \Delta^{\text{tol}}$, terminate;
   - if $\Delta_N(\mu) > \Delta^{\text{tol}}$ or $\beta_N^{\text{LB}}(\mu) \leq 0$ then set $k \leftarrow k + 1$ and go to 2.

In words, we first choose the reduced basis model associated with the nearest anchor point (in the Euclidean norm[7]) to compute $u_N(\mu)$ and $\Delta_N(\mu)$. If the error bound evaluation fails due to a negative inf-sup lower bound or the error bound is greater than the desired tolerance, then we choose the reduced basis model associated with the next nearest anchor point. We repeat the process until the error bound evaluation succeeds; assuming the offline training set is sufficiently rich, the algorithm identifies the appropriate subdomain and terminates after a few iterations (typically one).

5. Numerical Results.

5.1. Model Problem: Laterally Heated Cavities. We assess the effectiveness of our space-time certified reduced formulation using a laterally heated cavity flow governed by the Boussinesq equations. The spatial domain of interest is $\Omega = [0, 4] \times [0, 1]$; the domain is normalized by its height h, and is characterized by the aspect ratio $a = 4$. The (normalized) Boussinesq equations in $\mathbb{R}^2$ are given by

$$\begin{aligned}
\frac{\partial w_1}{\partial t} + \sum_{j=1}^{2} \sqrt{\text{Gr}} \frac{\partial w_j w_1}{\partial x_j} + \sqrt{\text{Gr}} \frac{\partial p}{\partial x_1} - \sum_{j=1}^{2} \frac{\partial^2 w_1}{\partial x_j \partial x_j} &= 0 \\
\frac{\partial w_2}{\partial t} + \sum_{j=1}^{2} \sqrt{\text{Gr}} \frac{\partial w_j w_2}{\partial x_j} + \sqrt{\text{Gr}} \frac{\partial p}{\partial x_2} - \sum_{j=1}^{2} \frac{\partial^2 w_2}{\partial x_j \partial x_j} - \sqrt{\text{Gr}}\, w_3 &= 0 \\
\frac{\partial w_3}{\partial t} + \sum_{j=1}^{2} \sqrt{\text{Gr}} \frac{\partial w_j w_3}{\partial x_j} - \sum_{j=1}^{2} \frac{1}{\text{Pr}} \frac{\partial^2 w_3}{\partial x_j \partial x_j} &= 0 \\
\frac{\partial w_1}{\partial x_1} + \frac{\partial w_2}{\partial x_2} &= 0,
\end{aligned}$$

where w_1 and w_2 are the velocities in the x_1 and x_2 directions respectively, w_3 is the temperature, p is the pressure, $\text{Gr} \equiv qah^4 g\beta/(k\nu^2)$ is the Grashof number, and $\text{Pr} \equiv \nu/\kappa$ is the Prandtl number. The scales used for time, length, velocity, pressure, and temperature are h^2/ν, h, $\sqrt{\text{Gr}}\nu/h$, $\rho\nu^2/h^2$, and qah/k, respectively.[8] The fluid properties are viscosity ν, density ρ, conductivity k, thermal diffusivity κ, and thermal expansion coefficient β. The heat flux along Γ_2 is denoted by q, and the gravitational

[7] A different norm may be employed if a better metric for defining the "closeness" of two parameters are known *a priori*.

[8] This particular temperature scaling ensures that, for a given Grashof number, the flow behavior for the fixed-heat-flux case considered in this work is understood loosely in terms of the fixed-temperature-difference case that has been extensively studied by, for example, Gelfgat *et al.* [11]

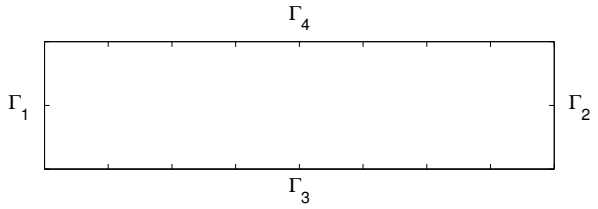

FIG. 5.1. *Boundary specification for the laterally heated cavity flow.*

acceleration is g. The boundary conditions are given by

$$\begin{aligned} w_1 = w_2 = 0 \quad &\text{on } \partial\Omega, \\ w_3 = 0 \quad &\text{on } \Gamma_1, \\ \frac{\partial w_3}{\partial n} = 0 \quad &\text{on } \Gamma_3 \text{ and } \Gamma_4, \\ \frac{\partial w_3}{\partial n} = \frac{1}{a} \quad &\text{on } \Gamma_2, \end{aligned}$$

where the boundaries are identified in Figure 5.1. The unsteady Boussinesq equations are integrated from $t = 0$ to $t = T = 0.5$. Because we employ the viscous time scale, $T = 0.5$ corresponds to many convective time units in a high Grashof number case.

We take the Grashof number as the parameter of interest and fix the Prandtl number to $\mathrm{Pr} = 0.015$. In particular, we wish to estimate the change in the velocity and thermal field as a function of the Grashof number; the pressure is not of interest in this work. Finally, we choose the space-time average temperature on the right boundary as our output, i.e.

$$\ell(w) = \frac{1}{T|\Gamma_2|} \int_I \int_{\Gamma_2} w_3 dx dt. \tag{5.1}$$

We will shortly verify that this is a bounded functional in our space-time setting.

5.2. Variational Formulation. To recast the Boussinesq equations in a weak form, we identify the function space V of the abstract formulation in Section 2.1 with the space of temperature and divergence-free velocity, i.e.

$$V \equiv \left\{ ((w_1, w_2), w_3) \in [H_0^1(\Omega)]^2 \times H^1(\Omega) : \frac{\partial w_1}{\partial x_1} + \frac{\partial w_2}{\partial x_2} = 0,\ w_3|_{\Gamma_D} = 0 \right\}.$$

In particular, as our interest is in the approximation of the velocity field and the temperature field — and not the pressure field — we consider formulation in explicitly divergence-free space. We recast the parametrized Boussinesq equations in a general form of Eq. (2.2) by identifying the spatial forms as follows:

$$\begin{aligned} a_0(w, v) &= \int_\Omega \sum_{j=1}^{2} \left[\frac{\partial v_1}{\partial x_j} \frac{\partial w_1}{\partial x_j} + \frac{\partial v_2}{\partial x_j} \frac{\partial w_2}{\partial x_j} + \frac{1}{\mathrm{Pr}} \frac{\partial v_3}{\partial x_j} \frac{\partial w_3}{\partial x_j} \right] dx, \qquad \Theta_0^a(\mu) = 1, \\ a_1(w, v) &= \int_\Omega v_2 w_3 dx, \qquad \Theta_1^a(\mu) = -\sqrt{\mu_1}, \\ c_1(w, z, v) &= -\frac{1}{2} \int_\Omega \sum_{i=1}^{3} \sum_{j=1}^{2} \frac{\partial v_i}{\partial x_j} \left(w_i z_j + z_i w_j \right) dx, \qquad \Theta_1^c(\mu) = \sqrt{\mu_1}, \end{aligned}$$

where $\mu_1 = \mathrm{Gr}$ is the Grashof number. Note that $\Theta_1^c : \mathcal{D} \to \mathbb{R}$ enters the continuity condition of the BRR error bound. The trilinear form is symmetric in the first two arguments and satisfies the boundedness assumption Eq. (2.3) with $C^{c_1} = 1$, i.e.

$$|c_1(w,z,v)| = \left| \frac{1}{2} \int_\Omega \sum_{i=1}^{3} \sum_{j=1}^{2} \frac{\partial v_i}{\partial x_j} \left(w_i z_j + z_i w_j \right) dx \right| \leq \|w\|_{L^4(\Omega)} \|z\|_{L^4(\Omega)} \|v\|_V,$$

where the $L^4(\Omega)$ norm for the vector field is as specified in Section 2.1. Thus, the above weak formulation of the Boussinesq equations conforms to the abstract formulation of Section 2.1.

The dual norm of the output functional Eq. (5.1) is bounded by

$$\|\ell\|_{\mathcal{X}'}^2 = \sup_{w \in \mathcal{X}_\delta} \frac{\left(\frac{1}{T|\Gamma_2|} \int_I \int_{\Gamma_2} w_3 dx dt \right)^2}{\|w\|_{\mathcal{X}_\delta}^2} \leq \sup_{w \in \mathcal{X}_\delta} \frac{\frac{1}{T|\Gamma_2|} \int_I \int_{\Gamma_2} w_3^2 dx dt}{\frac{1}{\mathrm{Pr}} \int_I \int_\Omega \nabla w_3 \cdot \nabla w_3 dx dt} = \frac{4\mathrm{Pr}}{T|\Gamma_2|},$$

where the inequality follows from $\|w\|_{\mathcal{X}_\delta}^2 \geq \|w\|_{L^2(I;V)}^2 \geq \frac{1}{\mathrm{Pr}} \|w_3\|_{L^2(I;H^1(\Omega))}^2$ and the last equality follows from recognizing the supremizer is $w_1 = w_2 = 0$, $w_3 = x$ (and its scalar multiples). For the particular laterally heated flows of interest, the upper bound of the dual norm evaluates to $\|\ell\|_{\mathcal{X}_\delta'} \approx 0.3464$.

5.3. Finite Element Discretization. We use $\mathbb{P}^2$-$\mathbb{P}^1$ Taylor-Hood elements for our finite element approximation. Namely, our discrete spatial approximation space is

$$V_h \equiv \left\{ w \in V : w|_\kappa \in [\mathbb{P}^2(\kappa)]^3,\ \kappa \in \mathcal{T}_h;\ \int_\Omega \nabla \cdot w q dx, \forall q \in Q_N \right\}, \tag{5.2}$$

where $Q_N = \{ q \in Q : q|_\kappa \in \mathbb{P}^1(\kappa),\ \kappa \in \mathcal{T}_h;\ \int_\Omega q dx = 0 \}$. Conceptually, it is straightforward to consider the divergence-free space for the evaluation of the finite element solution and the associated reduced-basis pieces: the dual norm of the residual, the inf-sup constant, and the Sobolev embedding constant. Of course, in practice, we impose the divergence free condition using Lagrange multipliers; the computational detail is summarized in Appendix A. The finite element discretization contains approximately 8,300 spatial degrees of freedom. We employ the $\mathbb{P}^2$ discontinuous Galerkin discretization for temporal integration with $K = 32$ time steps. Thus, the total number of space-time degrees of freedom for our finite element discretization is $\mathcal{N} \approx 800{,}000$.

5.4. Results. We assess the ability of our space-time certified reduced basis formulation to approximate and certify the solution of the laterally heated cavity flow as the Grashof number is varied from 1 to 150,000. The flow behaviors for the Grashof number of 6,000, 100,000, and 150,000 are depicted in Figure 5.2. For each case, the figure shows streamlines and isotherms at the final time ($t = T$) as well as the velocity history at $(x, y) = (1.25, 0.73)$. At the Grashof number of 6,000, the flow exhibits little nonlinear behavior, as evident from straight and equispaced isotherms in Figure 5.2(a). At the Grashof number of 100,000, convection plays an important role in characterizing the flow, as shown in Figure 5.2(b); this is evident from the characteristic "S" shape in the isotherms. However, the flow reaches steady state after the initial transient. At the Grashof number of 150,000, the flow exhibits steady-periodic behavior, as shown in Figure 5.2(c).

For purposes of comparison, we note that the classical time-marching $L^2(\Omega)$ error bound [19, 16] is inadequate for the certification of the flow considered in this work.

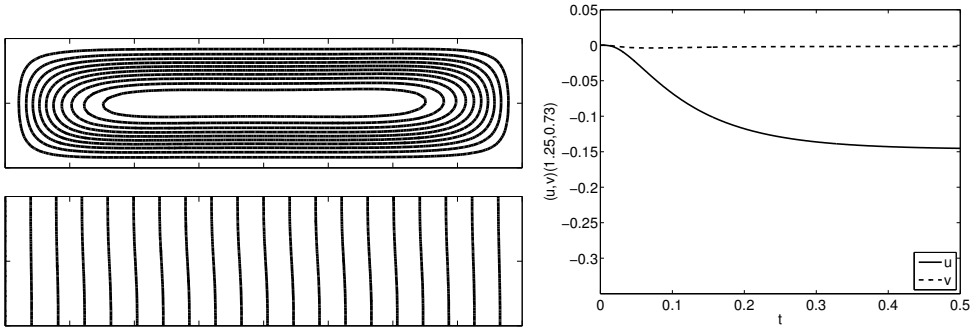

(a) Gr = 6,000

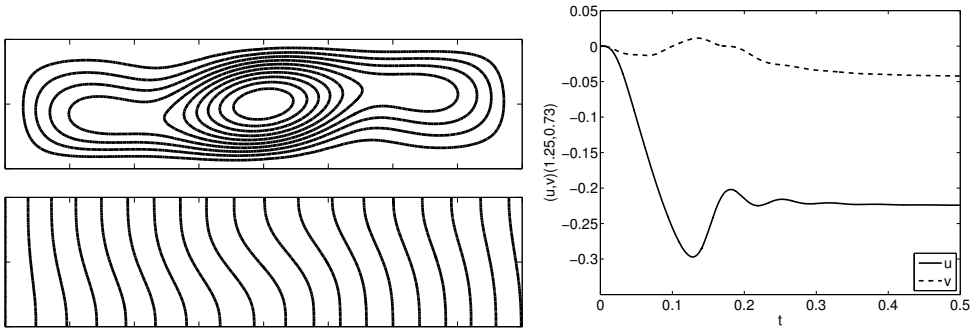

(b) Gr = 100,000

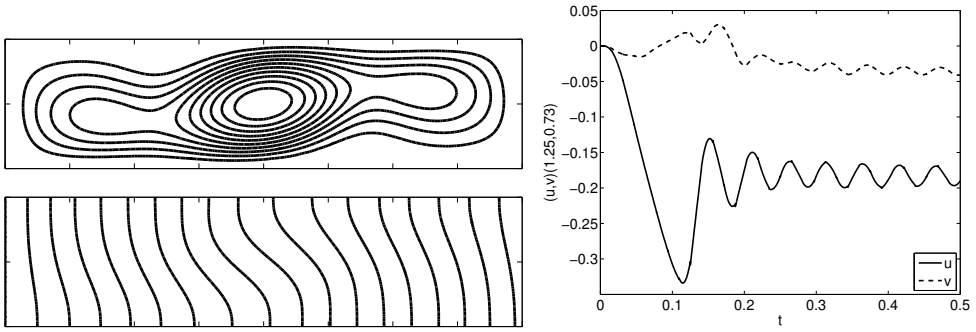

(c) Gr = 150,000

FIG. 5.2. *Streamlines at $t = T$ (top left), isotherms at $t = T$ (bottom left), and velocity history at $(x, y) = (1.25, 0.73)$ (right) for three different values of the Grashof number. The streamlines corresponds to evenly divided stream function values within each figure, and the isotherms are in increments of 0.05.*

The parameter that dictates the growth of the time-marching $L^2(\Omega)$ error bound is

the stability constant[9]

$$\omega(t) \equiv \inf_{v \in V_h} \frac{a_0(v,v) + 2\sum_{q=1}^{Q^a} a_q(v,v;\mu) + 4\sum_{q=1}^{Q^c} c_q(v,u_\delta(t),v;\mu)}{\|v\|^2_{L^2(\Omega)}} \; ;$$

it can be shown that, in the limit of $\Delta t \to 0$ by considering the continuous evolution equation, the time-marching $L^2(\Omega)$ error bound takes the form $\|e(T)\|^2_{L^2(\Omega)} \lesssim \epsilon^2_{V'} \omega^{-1}(-\exp(-\omega T)+1)$, where $\epsilon^2_{V'}$ is the $L^2(I)$ integral of the dual norm of the spatial residual.[10] The stability constant ω associated with the steady-state solutions of the Gr = 20,000, 30,000, and 40,000 flows are, respectively, $\omega \approx -48$, -380, and -1300; the associated amplification factors for $T = 0.5$ are $\omega^{-1}(-\exp(-\omega T)+1) \approx 5 \times 10^8$, 10^{79}, and 10^{284}. We observe that even if the residual is small, the classical time-marching $L^2(\Omega)$ error bounds would be too pessimistic to be meaningful for Gr $\geq$ 30,000; thus, we will not consider the classical time-marching formulation in this work.

We now study the behavior of the space-time reduced basis approximation and the associated space-time error bounds. We apply the *hp*-adaptive sampling algorithm to the flow of interest. The algorithm parameters are set as follows: the training set Ξ is a set of 1,000 points equidistributed over $\mathcal{D} \equiv [1, 150{,}000]$; SCM sampling parameters are $\bar{\beta}_N^{\bar{\mu},\mathrm{LB,tol}} = 0.25$ and $\beta_N^{\mathrm{gap,tol}} = 0.25$; and the target error tolerance is $\Delta^{\mathrm{tol}} = 0.01$.

Figure 5.3 shows the result of applying the space-time certified reduced basis method to the laterally heated cavity flow. The *hp* adaptive reduced basis yields 25 partitions; the reduced basis dimension for each partition varies from three to six, as shown in Figure 5.3(a), and the total of 125 reduced basis functions span the entire parameter space. The reduced basis sample points are marked by circles.[11] Note that our space-time formulation requires a large number of finite element offline solves to cover the parameter domain, as the formulation only generates one reduced basis snapshot from each offline solve. This is unlike in the POD-Greedy approximation, in which a large number of spatial snapshots (and hence a large reduced basis space) may be generated from a single offline solve of the evolution equation.

Figure 5.3(b) shows the behavior of the inf-sup lower bound over the parameter domain. We observe a rapid decay of the inf-sup lower bound away from each anchor point, especially in the high Grashof number regime; the decay suggests significant variations in the space-time dynamics induced by a small change in the parameter. For this reason, a relatively large number of SCM anchor points (and hence small partitions) are used to maintain positive inf-sup lower bounds over the entire parameter domain.

Figure 5.3(c) shows the variation in the $\mathcal{X}_\delta$ error bound with the parameter. Note that while the target $\mathcal{X}_\delta$ error for the reduced order model is 0.01, the actual error bound is driven to a much lower value. This is precisely due to the limitation noted in Remark 3.6; the BRR error bound cannot certify a low-fidelity reduced basis approximation that does not meet the residual criterion Eq. (3.8). For example, for the worst case of Gr = 150,000, the constants in Eq. (3.11) of Remark 3.6 evaluate to $\beta_N^{\mathrm{LB}} \approx 0.0121$, $\Theta_1^c \approx 387$, $C^{c_1} = 1$, and $\rho = 0.5$. This yields the maximum certifiable

[9] The constant slightly differs from that in [16] due to the difference in the trilinear forms.

[10] To simplify the expression for the bound, we consider a case in which the stability factor ω is invariant in time; however, the analysis readily extends to a non-stationary ω.

[11] As noted in Section 4, a reduced basis sampling point sometimes falls outside of the final subdomain to which it is associated; this is due the change in the subdomain, which is implicitly defined by the positive (more precisely threshold) inf-sup constraint, with N.

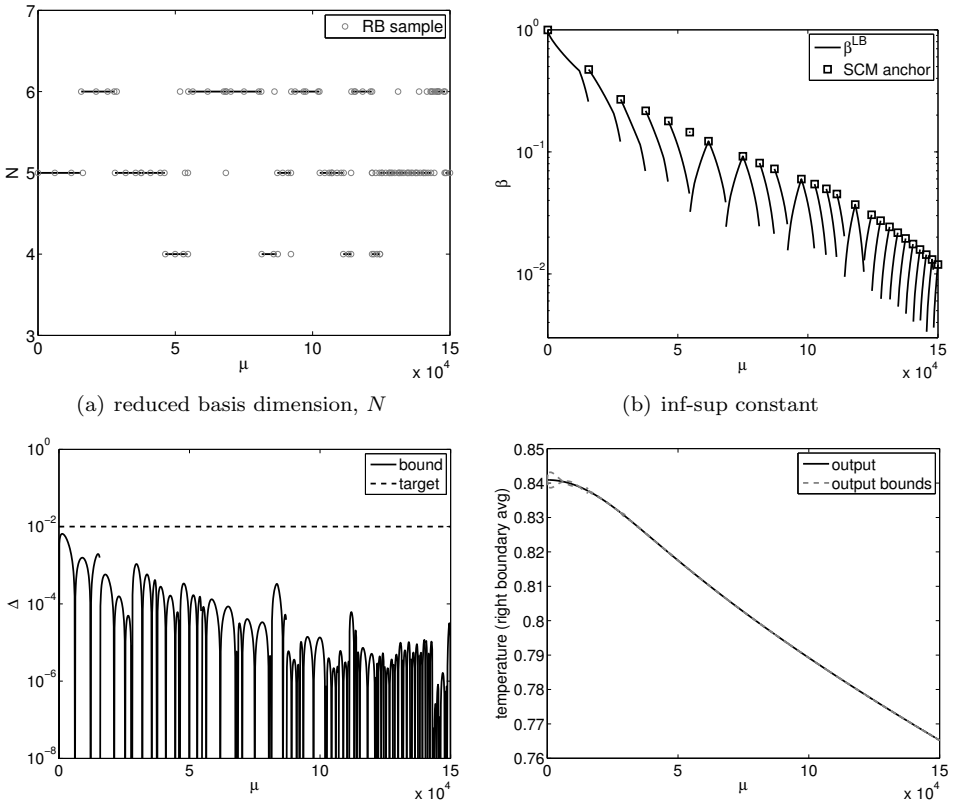

(a) reduced basis dimension, N

(b) inf-sup constant

(c) energy error bound, Δ_N

(d) output value and error bounds

FIG. 5.3. *Results of applying the space-time certified reduced basis method to the laterally heated cavity flow. (See the main text for descriptions.)*

error of approximately 6.25×10^{-5}, which is significantly smaller than the target error of 0.01. Nevertheless, the space-time formulation provides a certified reduced basis approximation of a high Grashof number (Gr = 150,000) flow that exhibits limited stability, a marked contrast to the classical time-marching $L^2(\Omega)$ error bound that becomes meaningless for the Grashof number over 30,000.

Figure 5.3(d) shows the variation in the time-integrated average temperature on the right boundary and associated error bound with the Grashof number. As the convection effect becomes more dominant, the temperature decreases for the constant heat-flux configuration considered. Note that the output error bound is very tight; recall that the output error bound is approximately 0.3464 times the $\mathcal{X}_\delta$ error bound shown in Figure 5.3(c).

Lastly, let us make a few comments regarding the offline and online computational performance of the certified reduced basis method.[12] For the Gr = 150,000 case, the solution of the finite element discretization with $\mathcal{N} \approx 800{,}000$ degrees of freedom requires about 520 seconds. The certified reduced basis method requires, in

[12]The research code developed in this work is a hybrid of Matlab and C (via mex) and is not optimized for computational performance. However, we believe the relative speed up achieved by the certified reduced basis method here is indicative of the relative speed up that would be observed in comparing optimized finite element and reduced basis codes.

the online stage, about 0.016 seconds to generate a reduced basis approximation and an associated error bound of less than 10^{-5} in the $\mathcal{X}_\delta$-norm; the rapid computation in the online stage is due to the space-time formulation whose online cost is independent of the number of time steps. On the other hand, the space-time formulation requires a significant computational effort in the offline stage, as the method requires not only a large number (in this particular case 125) truth solves but also computation of various space-time eigenproblems that, even with the time-marching procedures described in Section 3.4.2, are still computationally intensive.

6. Conclusions. We considered a certified reduced basis method for long-time integration of parametrized PDEs with quadratic nonlinearity that exhibit limited stability (non-coercive). We incorporated several new components to the previous work on space-time certification [25, 28]: a DG-in-time discretization and the associated norms that provide favorable stability properties; an *hp* Petrov-Galerkin reduced basis approximation that offers guaranteed stability; a variant of the natural norm SCM with considerations for the nonlinear equation and an associated efficient space-time computational strategy; and an *hp* sampling strategy for the nonlinear equation with limited stability. We applied the method to the unsteady Boussinesq equations that exhibit qualitatively different responses as the Grashof number increases: from a Stoke-like smooth transition to a steady-periodic response. We demonstrated that rigorous long-time *a posteriori* error bounds are possible for unstable hydrodynamic systems — systems that could not be certified with the classical time-marching $L^2(\Omega)$ error bounds; the method is able to rigorously confirm that changes in flow regime are not the result of an overly truncated low-order model, which is a demonstrated danger in a reduced-order approximation of unsteady flows [7].

We have however observed a number of limitations of the space-time formulation; we now reiterate on these points and propose future work. First, the space-time approach requires a large offline computational effort due to the small dimension of the reduced basis space constructed from a single truth solve compared to, say, POD-Greedy approach; future work will consider incorporation of a POD-Greedy approximation within the space-time certification framework in particular as regard the inf-sup (lower bound) calculation. Second, the BRR formulation, while providing rigorous bounds for nonlinear equations, places a very stringent requirement on the size of the normalized residual; while this limitation might be difficult to mitigate from a purely computational perspective, we will consider if in particular target applications — for example an estimation or controls — this effect can be mitigated through the incorporation of data. Lastly, we note that the substantial offline cost prohibits the treatment of significant variations in many parameters; however, an interpretation of the space-time variational formulation [27] provides a framework to demonstrate stability with respect to (very) small disturbances of potentially high dimensionality (for example, in initial conditions): the interpretation relies on BRR and the space-time inf-sup (and the associated computational strategy) introduced in this work.

Acknowledgments. I would like to thank Prof. Anthony Patera for the insightful discussions and many contributions throughout the development of this work. I would also like to thank Prof. Karsten Urban for initiating this research project in space-time approximation and error estimation. I would also like to thank Prof. Yvon Maday for his helpful comments on L^2-$\mathcal{X}$ and L^4-$\mathcal{X}$ embedding. This work was supported by OSD/AFOSR/MURI Grant FA9550-09-1-0613 and ONR Grant N00014-11-1-0713.

Appendix A. Computation in the Divergence-Free Space. In this appendix, we present details regarding computation in the divergence-free space approximated by $\mathbb{P}^2$-$\mathbb{P}^1$ Taylor-Hood elements, Eq. (5.2). As our objective is to illustrate the divergence-free aspect of the computational procedure, we consider the Stokes equations: find $u \in \mathcal{X}$ such that

$$\partial\mathcal{G}(u,v) = \dot{\mathcal{M}}_\delta(u,v) + \mathcal{A}(u,v) = \mathcal{F}(v), \quad \forall v \in \mathcal{Y} \ ;$$

the extension to the multi-parameter Boussinesq equations is straightforward.

Let $\{\chi_j\}_{j=1}^{n_v}$ be (vector-valued) $\mathbb{P}^2$ spatial basis for the velocity field and $\{\upsilon_j\}_{j=1}^{n_p}$ be $\mathbb{P}^1$ spatial basis for the pressure field. The spatial velocity mass matrix $\boldsymbol{m}_s \in \mathbb{R}^{n_v \times n_v}$, the velocity Laplacian matrix $\boldsymbol{a} \in \mathbb{R}^{n_v \times n_v}$, the divergence-free constraint matrix $\boldsymbol{b} \in \mathbb{R}^{n_v \times n_p}$, and the load vector $\boldsymbol{f} \in \mathbb{R}^{n_v}$ are given by

$$\boldsymbol{m}_{s,ij} \equiv (\chi_j, \chi_i)_{L^2(\Omega)}, \quad \boldsymbol{a}_{ij} \equiv a(\chi_j, \chi_i) = \int_\Omega \frac{\partial \chi_i}{\partial x_k}\frac{\partial \chi_j}{\partial x_k} dx$$
$$\boldsymbol{b}_{ij} \equiv b(\upsilon_j, \chi_i) = -\int_\Omega \frac{\partial \chi_i}{\partial x_i}\upsilon_j dx, \quad \boldsymbol{f}_i \equiv f(\chi_i) \ .$$

We then introduce $(n_v + n_p) \times (n_v + n_p)$ expanded spatial matrices and a $(n_v + n_p)$ expanded vector

$$\tilde{\boldsymbol{m}}_s \equiv \begin{bmatrix} \boldsymbol{m} & 0 \\ 0 & 0 \end{bmatrix}, \quad \tilde{\boldsymbol{a}} \equiv \begin{bmatrix} \boldsymbol{a} & 0 \\ 0 & 0 \end{bmatrix}, \quad \tilde{\boldsymbol{b}} \equiv \begin{bmatrix} 0 & \boldsymbol{b} \\ \boldsymbol{b}^T & 0 \end{bmatrix}, \quad \text{and} \quad \tilde{\boldsymbol{f}} = \begin{bmatrix} \boldsymbol{f} \\ 0 \end{bmatrix} \ .$$

Note that $\tilde{\boldsymbol{a}} + \tilde{\boldsymbol{b}}$ is the standard saddle-point matrix associated with the steady-state discretization of the Stokes equations by the Taylor-Hood elements.

Let $\{\sigma^j\}_{j=1}^{n_t}$, $n_t \equiv (p+1)K$, be temporal DG basis. The temporal mass matrix $\boldsymbol{m}_t \in \mathbb{R}^{n_t \times n_t}$, the evolution matrix $\dot{\boldsymbol{m}}_t \in \mathbb{R}^{n_t \times n_t}$, and the initial condition matrix $\boldsymbol{m}_{t_0} \in \mathbb{R}^{n_t \times n_t}$ are given by

$$\boldsymbol{m}_{t,ij} \equiv \int_I \sigma^i(t)\sigma^j(t) dt$$
$$\dot{\boldsymbol{m}}_{t,ij} \equiv \sum_{k=1}^K \int_{I^k} \sigma^i(t)\frac{\partial \sigma^j(t)}{\partial t} dt + \sum_{k=1}^{K-1} \sigma^i(t_+^k)(\sigma^j(t_+^k) - \sigma^j(t_-^k))$$
$$\boldsymbol{m}_{t_0,ij} \equiv \sigma^i(t_+^0)\sigma^j(t_+^0) \ .$$

These matrices may be tensorized to emphasize their block structures; for instance, by introducing reference elemental basis $\{\xi_j\}_{j=1}^{p+1}$, by forming a $(p+1)\times(p+1)$ reference elemental matrix $\boldsymbol{m}_{e,ij} \equiv \int_0^1 \xi_i(t)\xi_j(t)dt$, and by introducing a diagonal scaling matrix $\boldsymbol{d}_t = \text{diag}(\Delta t^1, \ldots, \Delta t^K) \in \mathbb{R}^K$, we have $\boldsymbol{m}_t = \boldsymbol{d}_t \otimes \boldsymbol{m}_e$. While we take advantage of this tensorization in our implementation, for notational simplicity, we will not use the tensorized form for the presentation here.

We now introduce the "forward" space-time operator associated with the bilinear form $\partial\mathcal{G}$ that acts on the velocity-pressure space

$$\widetilde{\mathbf{G}} = \dot{\boldsymbol{m}}_t \otimes \tilde{\boldsymbol{m}}_s + \boldsymbol{m}_t \otimes \tilde{\boldsymbol{a}} + \boldsymbol{m}_{t_0} \otimes \tilde{\boldsymbol{m}}_s \ .$$

The corresponding "inverse" operator that appropriately enforces the divergence-free constraint is

$$\widetilde{\mathbf{G}}_c^{-1} = (\widetilde{\mathbf{G}} + \boldsymbol{m}_t \otimes \tilde{\boldsymbol{b}})^{-1}$$

Then, the space-time finite element coefficient vector $\tilde{\boldsymbol{u}} \in \mathbb{R}^{K(p+1)(n_v+n_p)}$ such that $u(t,x) = \tilde{\boldsymbol{u}}_i^k \sigma^k(t)\chi_i(x)$ and $p(t,x) = \tilde{\boldsymbol{u}}_{n_v+i}^k \sigma^k(t)\upsilon_i(x)$ is the solution of

$$\widetilde{\mathbf{G}}_c \tilde{\boldsymbol{u}} = \widetilde{\mathbf{F}} \ ,$$

where the load vector is given by $\widetilde{\mathbf{F}} = \boldsymbol{m}_t \otimes \tilde{\boldsymbol{f}}$. Note that $\tilde{\boldsymbol{f}}$ (and hence $\widetilde{\mathbf{F}}$) has zeros for the entries corresponding to the continuity equation and $\tilde{\boldsymbol{b}}$ (and hence $\boldsymbol{m}_t \otimes \tilde{\boldsymbol{b}}$) has the divergence operator for the entries corresponding to the continuity equation; together, they enforce the divergence-free constraint. We emphasize that $\widetilde{\mathbf{G}}_c$ operates on the velocity-pressure space (i.e. the velocity-Lagrange-multiplier space) of the dimension $\mathbb{R}^{K(p+1)(n_v+n_p)}$ and is different from the operator $\mathbf{G}$ in Sections 3.4.2 and 3.5 that operates on the divergence free space; however, the application of $\widetilde{\mathbf{G}}_c^{-1}$ onto a vector with zeros for the continuity equation produces the result of applying $\mathbf{G}^{-1}$ in the divergence free-space.

Similarly, all the action of the $\mathbf{Y}$, $\mathbf{Y}^{-1}$, $\mathbf{X}$, and $\mathbf{X}^{-1}$ operators that appear in Sections 3.4.2 and 3.5 are accomplished by using the following expanded velocity-pressure matrices:

$$\widetilde{\mathbf{Y}} = \boldsymbol{m}_t \otimes \tilde{\boldsymbol{a}} + \boldsymbol{m}_{t_0} \otimes \tilde{\boldsymbol{m}}_s, \quad \widetilde{\mathbf{Y}}_c^{-1} = (\widetilde{\mathbf{Y}} + \boldsymbol{m}_t \otimes \tilde{\boldsymbol{b}})^{-1},$$
$$\widetilde{\mathbf{X}} = \widetilde{\mathbf{G}}_{\text{heat}}^T \widetilde{\mathbf{Y}}_c^{-1} \widetilde{\mathbf{G}}_{\text{heat}}, \quad \widetilde{\mathbf{X}}_c^{-1} = (\widetilde{\mathbf{G}}_{\text{heat}} + \boldsymbol{m}_t \otimes \boldsymbol{b})^{-1} \widetilde{\mathbf{Y}} (\widetilde{\mathbf{G}}_{\text{heat}} + \boldsymbol{m}_t \otimes \boldsymbol{b})^{-T} \ .$$

For instance, we may express the inf-sup eigenproblem Eq. (3.28) using the space-time expanded matrices: Find $(\tilde{\boldsymbol{w}}, \lambda) \in \mathbb{R}^{n_v+n_p} \times \mathbb{R}$ such that

$$\widetilde{\mathbf{G}}_c \widetilde{\mathbf{Y}}_c^{-1} \widetilde{\mathbf{G}}_c \tilde{\boldsymbol{w}} = \lambda \widetilde{\mathbf{X}} \tilde{\boldsymbol{w}} \ .$$

The generation of an effective Krylov space for the minimum eigenvalue is accomplished by $\tilde{\boldsymbol{v}} \leftarrow \widetilde{\mathbf{G}}_c^{-1} \widetilde{\mathbf{Y}} \widetilde{\mathbf{G}}_c^{-T} \widetilde{\mathbf{X}} \tilde{\boldsymbol{v}}$; the resulting Krylov space is clearly divergence-free. (Alternatively, $\tilde{\boldsymbol{v}} \leftarrow \widetilde{\mathbf{G}}_c^{-1} \widetilde{\mathbf{Y}}_c \widetilde{\mathbf{G}}_c^{-T} \widetilde{\mathbf{X}} \tilde{\boldsymbol{v}}$ can be used. Up to rounding errors, the two velocity spaces are identical; however, the pressure approximations are different (which does not affect the inf-sup constant in our context).)

Appendix B. List of Variables. Table B.1 provides a list of select variables used in this work and their short descriptions. Not all variables are listed; the list is limited to those variables that appear across multiple subsections and in particular those used in the description of the *hp*-adaptive sampling algorithm in Section 4.

REFERENCES

[1] M. Barrault, Y. Maday, N. C. Nguyen, and A. T. Patera, *An "empirical interpolation" method: application to efficient reduced-basis discretization of partial differential equations*, C. R. Acad. Sci. Paris, Ser. I, 339 (2004), pp. 667–672.

[2] C. Bottasso, *A new look at finite elements in time: a variational interpretation of runge-kutta methods*, Appl. Numer. Math., 25 (1997), pp. 355–368.

[3] F. Brezzi, J. Rappaz, and P. A. Raviart, *Finite dimensional approximation of nonlinear problems. part I: Branches of nonsingular solutions*, Numer. Math., 36 (1980), pp. 1–25.

[4] C. Canuto, T. Tonn, and K. Urban, *A poseteriori error analysis of the reduced basis method for nonaffine parametried nonlinear PDEs*, SIAM J. Numer. Anal., 47 (2009), pp. 2001–2022.

[5] F. Casenave, *Accurate a posteriori error evaluation in the reduced basis method*, C. R. Acad. Sci. Paris, Ser. I, (2012), pp. 539–542.

[6] F. Casenave, A. Ern, and T. Leliévre, *Accurate and efficient evaluation fo the a posteriori error estimator in the reduced basis method*, Math. Model. Numer. Anal., (submitted).

variable	description
$\mathcal{G}(\cdot,\cdot;\cdot)$, $\mathcal{G}_\delta(\cdot,\cdot;\cdot)$	space-time semilinear form (continuous/discrete)
$\partial\mathcal{G}(\cdot,\cdot,\cdot;\cdot)$, $\partial\mathcal{G}_\delta(\cdot,\cdot,\cdot;\cdot)$	space-time linearized form (continuous/discrete)
$\mathcal{F}(\cdot;\cdot)$, $\mathcal{A}(\cdot,\cdot;\cdot)$, $\mathcal{C}(\cdot,\cdot,\cdot;\cdot)$	space-time parametrized linear, bilinear, and trilinear forms
$\mathcal{F}_q(\cdot)$, $\mathcal{A}_q(\cdot,\cdot)$, $\mathcal{C}_q(\cdot,\cdot,\cdot)$	μ-independent space-time forms for affine expansion
$\Theta_q^f(\cdot)$, $\Theta_q^a(\cdot)$, $\Theta_q^c(\cdot)$	μ-dependent functions for affine expansion
Q^f, Q^a, Q^c	number of terms in affine expansion
Ξ	reduced basis training points
N	dimension of the space-time reduced basis space
$u_\delta(\mu)$	finite element approximation
$u_N(\mu)$	reduced basis approximation
$\beta_N(\mu)$	inf-sup constant for $\partial\mathcal{G}_\delta(\cdot, u_N(\mu), \cdot;\mu)$
$\beta_N^{\mathrm{LB}}(\mu)$	a lower bound of $\beta_N(\mu)$
$\bar\beta_N^{\bar\mu}(\mu)$	inf-sup constant correction factor about $\bar\mu$
$\bar\beta_N^{\bar\mu,\mathrm{LB}}(\mu)$, $\bar\beta_N^{\bar\mu,\mathrm{UB}}(\mu)$	a lower/upper bound of $\bar\beta_N^{\bar\mu}(\mu)$
$\bar\mu$	SCM anchor point
$B^{\bar\mu}$	SCM bounding box
M^{SCM}	SCM control points
Z_N^{LB}, Z_N^{UB}	SCM set for evaluation of $\bar\beta_N^{\bar\mu,\mathrm{LB}}(\mu)$, $\bar\beta_N^{\bar\mu,\mathrm{UB}}(\mu)$
$\bar\beta_N^{\bar\mu,\mathrm{LB,tol}}$, $\beta_N^{\mathrm{gap,tol}}$	SCM threshold parameters
$\epsilon_N(\mu)$	residual dual norm
$\gamma(\mu)$	continuity constant for the trilinear form $\mathcal{C}$
ρ	$L^4(I;L^4(\Omega))$-$\mathcal{X}_\delta$ Sobolev embedding constant
$\tau_N(\mu)$	BRR normalized residual
$\Delta_N(\mu)$	error bound
Δ^{tol}	error bound tolerance

TABLE B.1
List of select variables and their brief descriptions.

[7] J. H. Curry, J. R. Herring, J. Loncaric, and S. A. Orszag, *Order and disorder in two- and three-dimensional bénard convection*, J. Fluid Mech., 147 (1984), pp. 1–38.

[8] S. Deparis, *Reduced basis error bound computation of parameter-dependent Navier-Stokes equations by the natural norm approach*, SIAM J. Numer. Anal., 46 (2008), pp. 2039–2067.

[9] J. L. Eftang, A. T. Patera, and E. M. Rønquist, *An "hp" certified reduced basis method for parametrized elliptic partial differential equations*, SIAM J. Sci. Comput., 32 (2010), pp. 3170–3200.

[10] K. Eriksson and C. Johnson, *Error estimates and automatic time step control for nonlinear parabolic problems, I*, SIAM J. Numer. Anal., 24 (1987), pp. 12–23.

[11] A. Y. Gelfgat, P. Z. Bar-Yoseph, and A. L. Yarin, *Stability of multiple steady states of convection in laterally heated cavities*, J. Fluid Mech., 388 (1999), pp. 315–334.

[12] M. A. Grepl and A. T. Patera, *A posteriori error bounds for reduced-basis approximations of parametrized parabolic partial differential equations*, Math. Model. Numer. Anal., 39 (2005), pp. 157–181.

[13] B. Haasdonk and M. Ohlberger, *Reduced basis method for finite volume approximations of parametrized linear evolution equations.*, Math. Model. Numer. Anal., 42 (2008), pp. 277–302.

[14] D. B. P. Huynh, D. J. Knezevic, Y. Chen, J. S. Hesthaven, and A. T. Patera, *A natural-norm successive constraint method for inf-sup lower bounds*, Comput. Methods Appl. Mech. Engrg., 199 (2010), pp. 1963–1975.

[15] P. Jamet, *Galerkin-type approximations which are discontinuous in time for parabolic equations in a variable domain*, SIAM J. Numer. Anal., 15 (1978), pp. 912–928.

[16] D. J. Knezevic, N.-C. Nguyen, and A. T. Patera, *Reduced basis approximation and a posteriori error estimation for the parametrized unsteady Boussinesq equations*, Math.

Mod. Meth. Appl. S., 21 (2011), pp. 1415–1442.
[17] Y. Maday. Private communication, Dec. 2012.
[18] Y. Maday, A. T. Patera, and D. V. Rovas, *A blackbox reduced-basis output bound method for noncoercive linear problems*, in Studies in Mathematics and its Applications, D. Cioranescu and J. L. Lions, eds., Elsevier Science B. V., 2002, pp. 533–569.
[19] N.-C. Nguyen, G. Rozza, and A. T. Patera, *Reduced basis approximation and a posteriori error estimation for the time-dependent viscous Burgers' equation*, Calcolo, 46 (2009), pp. 157–185.
[20] A. Quarteroni and A. Valli, *Numerical Approximation of Partial Differential Equations*, Springer, New York, 1997.
[21] G. Rozza and K. Veroy, *On the stability of the reduced basis method for stokes equations in parametrized domains*, Comput. Methods Appl. Mech. Engrg., 196 (2007), pp. 1244–1260.
[22] C. Schwab and R. Stevenson, *Space-time adaptive wavelet methods for parabolic evolution problems*, Math. Comp., 78 (2009), pp. 1293–1318.
[23] S. Sen, K. Veroy, D. B. P. Huynh, S. Deparis, N. C. Nguyen, and A. T. Patera, *"Natural norm" a posteriori error estimators for reduced basis approximations*, J. Comput. Phys., 217 (2006), pp. 37–62.
[24] K. Urban and A. T. Patera, *An improved error bound for reduced basis approximation of linear parabolic problems*, Math. Comp., (2012), p. submitted.
[25] ———, *A new error bound for reduced basis approximation of parabolic partial differential equations*, C. R. Acad. Sci. Paris, Ser. I, 350 (2012), pp. 203–207.
[26] K. Veroy and A. T. Patera, *Certified real-time solution of the parametrized steady incompressible Navier-Stokes equations: rigorous reduced-basis a posteriori error bounds*, Internat. J. Numer. Methods Fluids, 47 (2005), pp. 773–788.
[27] M. Yano and A. T. Patera, *A space-time variational approach to hydrodynamic stability theory*, Proc. R. Soc. A, 469 (2013), p. Article Number 20130036.
[28] M. Yano, A. T. Patera, and K. Urban, *A space-time certified reduced basis method for Burgers' equation*, Math. Mod. Meth. Appl. S., (submitted).